Reaction kinetics of the destructive catalytic hydrogenation of quinoline
by James R Ryffel

A THESIS Submitted to the Graduate Faculty in partial fulfillment of the requirements for the degree of Doctor of Philosophy in Chemical Engineering
Montana State University

Abstract:
A great deal of Interest has been shown lately in the denitrogenatlon of shale oil stocks by catalytic hydrogenation. Most of the work has been on a purely empirical basis and little is known about the mechanism of the reaction since such, a complex system, is involved,. For this reason,- a study has been Carried out on the hydrogenation of a "synthetic shale oil" composed of quinoline and a hydrocarbon carrier oil. The objectives were the basic study of the kinetics of the reaction and mechanism involved with the idea that the work might eventually be of some value in the broader problem of upgrading shale oil-stocks.

The work was carried out on a bench—scale, continuous-flow, fixed-bed catalytic reactor system. The range of operating conditions were: temperature -725 to 800°F; pressure - 250 to 1000 psig; flow rate - l/3 to 10 g oil per g catalyst per hour; and initial nitrogen concentration -0.25 to 2.0 wt %N. A charge of 15 to 100 g of a cobalt-molybdate catalyst was used in the reactor and hydrogen flow rate was 7500 SCF/bbl.

Using vapor-phase chromatography analysis, it was found that the hydrogenation probably occurs in four reactions.; (1) addition of a hydrogen to quinoline to form dihydroquinoline (2) addition of a second hydrogen to. form tetrahydroquinoline, (3) cleavage of the nitrogen ring and addition of a third hydrogen to form o-propylaniline, and (4) addition of a fourth hydrogen to yield ammonia and a mixture of n-propylbengene and iso-propylbenzene. The fourth reaction was found to be the slowest or rate controlling reaction. Some side reactions were noted which gave small amounts of other aniline, benzene, and cyclohexane homologs.

Both film and internal diffusion effects were shown to be negligible. The reaction was found to follow pseudo first order reaction kinetics when a large excess of hydrogen was used.

Five mechanisms for the slowest reaction, were postulated. On the basis of the experimental data, all but one of the postulated controlling steps were rejected. The acceptable mechanism was the dual site surface reaction between adsorbed, o-propylaniline, and molecularly adsorbed hydro,-gen with the surface reaction itself being the rate controlling step.

It was noted that the initial rate of reaction increased with in- creasing temperature and pressure but went through a maximum with variable initial nitrogen Concentration. The energy of activation was calculated from the Arrhenius equation and found to vary from 23.6 to 33.7 Kcal/mole as a linear function of pressure.

REACTION KINETICS OF THE DESTRUCTIVE CATALYTIC HYDROGENATION OF QUINOLINE

by

JAMES R. RYFFEL

A THESIS

Submitted to the Graduate Faculty

in

partial fulfillment of the requirements

for the degree of

Doctor of Philosophy in Chemical Engineering

at

Montana State College

Approved:

Lloyd Berg
Head, Major Department

Lewis S Mayfield
Chairman, Examining Committee

Leon Johnson
Dean, Graduate Division

Bozeman, Montana
February, 1960

TABLE OF CONTENTS

ABSTRACT

A great deal of interest has been shown lately in the denitrogenation of shale oil stocks by catalytic hydrogenation. Most of the work has been on a purely empirical basis and little is known about the mechanism of the reaction since such a complex system is involved. For this reason, a study has been carried out on the hydrogenation of a "synthetic shale oil" composed of quinoline and a hydrocarbon carrier oil. The objectives were the basic study of the kinetics of the reaction and mechanism involved with the idea that the work might eventually be of some value in the broader problem of upgrading shale oil stocks.

The work was carried out on a bench-scale, continuous-flow, fixed-bed catalytic reactor system. The range of operating conditions were: temperature - 725 to 800°F; pressure - 250 to 1000 psig; flow rate - 1/3 to 10 g oil per g catalyst per hour; and initial nitrogen concentration - 0.25 to 2.0 wt % N. A charge of 15 to 100 g of a cobalt-molybdate catalyst was used in the reactor and hydrogen flow rate was 7500 SCF/bbl.

Using vapor-phase chromatography analysis, it was found that the hydrogenation probably occurs in four reactions: (1) addition of a hydrogen to quinoline to form dihydroquinoline, (2) addition of a second hydrogen to form tetrahydroquinoline, (3) cleavage of the nitrogen ring and addition of a third hydrogen to form o-propylaniline, and (4) addition of a fourth hydrogen to yield ammonia and a mixture of n-propylbenzene and iso-propylbenzene. The fourth reaction was found to be the slowest or rate controlling reaction. Some side reactions were noted which gave small amounts of other aniline, benzene, and cyclohexane homologs.

Both film and internal diffusion effects were shown to be negligible. The reaction was found to follow pseudo first order reaction kinetics when a large excess of hydrogen was used.

Five mechanisms for the slowest reaction were postulated. On the basis of the experimental data, all but one of the postulated controlling steps were rejected. The acceptable mechanism was the dual site surface reaction between adsorbed o-propylaniline, and molecularly adsorbed hydrogen with the surface reaction itself being the rate controlling step.

It was noted that the initial rate of reaction increased with increasing temperature and pressure but went through a maximum with variable initial nitrogen concentration. The energy of activation was calculated from the Arrhenius equation and found to vary from 23.6 to 33.7 Kcal/mole as a linear function of pressure.

I INTRODUCTION

Although the nation's known petroleum reserves are greater than ever before and have been increasing every year for several decades, the time will come when these reserves are exhausted. With this realization, technologists have been vitally concerned with processes whereby other fuels can be used to supplant petroleum products. Commercial utilization of atomic energy and solar energy will reduce the demand for hydrocarbon fuels but the increased application of hydrocarbons to other uses, e.g., petrochemicals, would appear to offset any reduction in demand for hydrocarbons in general.

Concerned with the increased consumption of petroleum and the need for a long-term supply of liquid fuels, the United States' Congress passed the Synthetic Liquid Fuels Act of 1944. This Act authorized research and development on new sources of oil, among which was shale oil (22). The United States' Bureau of Mines then proceeded to construct retorts and a demonstration mine near Rifle, Colorado (38).

As a supplement to petroleum for a source of hydrocarbons, oil from oil-shale appears to be one of the most promising raw materials at the present time. The upgraded products are very similar to those obtained from petroleum and there is a sufficiently abundant supply for many years. The principal deposits of oil-shale in the United States are located in a 16,500 square mile area of Colorado, Wyoming, and Utah called the Green River Formation (39). This bed of oil-shale contains an estimated 500 billion barrels of oil--about twice as much as the world's proven reserves of petroleum and 15 times the proven reserves of the United States (42,

46). For this reason, many companies, besides the United States Government, have shown interest in developing this oil-shale deposit.

Exploitation of oil shale may be divided into three steps:

1. Mining of the oil-shale.
2. Retorting of the mined shale to obtain crude shale oil.
3. Refining and upgrading the crude shale oil to produce marketable products.

The mining and retorting steps have been fairly well developed. However, there is much work to be done yet on the refining and upgrading of the crude shale oil.

The United States' Bureau of Mines at Rifle, Colorado, operates a room-and-pillar type of mining operation whereby about 75% of the oil-shale is removed; the remaining shale is left behind to serve as a roof support (22). The shale is then crushed and retorted as in the continuous gas combustion retort developed by the Union Oil Company (5, 22).

The crude shale oil and its distillates do not make satisfactory fuels because of high nitrogen and sulfur content, unsaturation, low octane, color instability, and gum formation properties (7, 15, 31). Initial treatment of the crude shale oil or distillates by conventional petroleum processing, e.g., catalytic cracking or reforming, has not proven particularly successful. The nitrogen compounds are strongly adsorbed on the catalysts, causing their rapid deactivation (2, 14, 30). In addition, the products are unstable, producing substantial quantities of gum and an objectionable color. The nitrogen compounds are also partially

responsible for the extensive gum formation in that they accelerate the oxidation of the numerous unsaturated compounds (41). Prior treatment to remove the nitrogen is thus necessary. However, severe chemical treatment such as acid washing is not satisfactory since this removes the olefins present as well as the nitrogen compounds themselves, thereby causing a considerable volume loss of product (29).

Destructive catalytic hydrogenation of the crude shale oil or shale oil fractions seems to be the most promising method for producing a stable material for further upgrading processes (8, 10, 11). By this method, the carbon-nitrogen bonds are broken yielding ammonia and hydrocarbons. In addition, the sulfur is similarly removed as hydrogen sulfide and olefin compounds are saturated. Thus the nitrogen and sulfur are removed and the olefins converted to paraffins, all in one operation.

The catalytic hydrogenation of shale oil fractions has been studied by the Chemical Engineering Department at Montana State College since 1954 (4, 19, 23, 28). They were interested in developing an economical process which would produce a low nitrogen and low sulfur content effluent oil to be used as a charge stock for conventional petroleum refining processes. Their research included studies of the effects of process variables such as temperature, pressure, space velocity, treat gas rate, and treat gas composition; studies of the efficiency and ability of twelve different catalysts in denitrogenation; and a kinetic study. Since the nitrogen removal is of primary importance, the sulfur removal and olefin saturation being done relatively easily, they were concerned mainly with correlating

their data to nitrogen removal.

Due to the complexity of shale oil and subsequently to the many thousands of reactions occurring simultaneously, they were unable to accomplish much in the kinetic study. They did determine that the controlling reaction was pseudo-first order with respect to the nitrogen in the charge stock and that the transfer of reactants to the catalyst by diffusion was not the rate controlling step in the reaction for the particular reactor used in the study.

A more thorough understanding of the kinetics and mechanism of the reactions involved in shale oil denitrogenation would be very desirable but this information is virtually impossible to obtain in such a complex system. Therefore, it was proposed to study the reactions involved in the destructive catalytic hydrogenation of a "synthetic shale oil", that is, an oil made up of a high molecular weight hydrocarbon and a single nitrogen compound characteristic of the type found in crude shale oil.

This thesis is a report of such an investigation. The information obtained is of a fundamental nature and should be of value in solving the broader problems of upgrading shale oil stocks.

II RESEARCH OBJECTIVES

The objectives of this research were simply to gather and evaluate the data from the destructive catalytic hydrogenation of a "synthetic shale oil" composed of a hydrocarbon carrier oil and a single nitrogen compound. Of primary concern was the study of the kinetics and mechanism of the reactions involved. We were interested in determining the following things:

1. The empirical order of reaction.
2. A suitable overall reaction mechanism and the rate controlling step. If this was not possible, at least elimination of unlikely mechanisms.
3. Constants for the Arrhenius equation and reaction rate constants at various process conditions.
4. The general effects of changing the process variables of temperature, pressure, oil flow rate, hydrogen flow rate, and nitrogen concentration.
5. The qualitative and quantitative identification of reaction products and intermediates.

In general, the above objectives were realized insofar as time and available equipment allowed. The research was meant to be of a fundamental nature but designed so that the results could be applied to the broader problem of upgrading crude shale oil stocks.

III EXPERIMENTAL CONSIDERATIONS

A. Introduction

Selection of Feedstock: In order to prepare the synthetic shale oil feedstock, it was necessary to find a high molecular weight hydrocarbon carrier oil and a nitrogen compound characteristic of those found in the crude shale oil. They had to be readily available in gallon lots at a reasonable price. In addition, it was desirable for the oil to: (1) have a boiling range above that of the expected reaction products and intermediates so that they could be readily separated by distillation, and (2) not be affected by the hydrogenation process itself. The nitrogen compound should also be sufficiently difficult to remove so that the processing conditions are relatively severe, corresponding to those used in normal shale oil processing.

The literature (1, 6, 38, 39, 41) reports that the nitrogen in shale oil exists as a constituent of heterocyclic molecules, primarily as homologs of pyridine, pyrrole, and quinoline. It was decided to use quinoline, available as a coal-tar by-product, for the source of nitrogen. The quinoline obtained was quite impure; however, the contaminants of isoquinoline and quinaldine were readily removed by distillation. The carrier oil chosen was "Peneteck", a commercial mineral oil produced by the Pennsylvania Refining Corporation. It is a clear white hydrocarbon oil produced from a naphthene-paraffin base petroleum crude. It contains essentially no aromatics or olefins, has a boiling range of 250-270°C and a density of .797 gm/cc. In addition, a small amount of pure cetane

(n-hexadecane) was obtained for use as a supplementary carrier oil.

Selection of Process Conditions: Using previous work and exploratory runs as a guide, the following ranges of operating conditions were selected:

Temperature:	725-800°F
Pressure:	250-1000 psig
Hydrogen Flow Rate:	2500-10,000 SCF/bbl
Nitrogen Concentration:	0.25-2.00 %N
Space Velocity:	0.33-10.0 gm oil/gm catalyst/hr.
Catalyst Amount:	15-100 gm

The criteria of these selections was the ability to control the degree of nitrogen conversion between 10% and 90% by proper adjustment of the process conditions chosen. Of course, these conditions had to be compatible with the limitations of the equipment involved and the analysis techniques used. In addition, it was necessary to ensure that there would be little or no effect on the carrier oil.

Thermodynamic Study: Before the initial work was begun, a thermodynamic study of the hydrogenation of quinoline was carried out. This was done to verify thermodynamically the feasibility of the overall reaction of quinoline and hydrogen to yield ammonia and propylbenzene. For example, the free energy changes and equilibrium constants at several temperatures are: at 500°K, ΔF° = -23,800 cal/g mole and $K_{eq} = 2.4 \times 10^{10}$; at 700°K, ΔF° = -10,100 cal/g mole and $K_{eq} = 1.4 \times 10^{3}$. The temperature of neutral equilibrium was calculated to be 850°K. These calculations indicated a favorable reaction. In addition, it was shown that a 98.9 percent equilibrium conversion could be expected at 700°K and 50 atm. pressure, condi-

tions representative of shale oil hydrogenation. The complete study, with calculations at four temperatures and four pressures, is included in the appendix.

B. Materials

Feedstock: The crude quinoline, containing approximately 90% quinoline and 10% iso-quinoline and quinaldine, was purified by fractionation in a one-meter column packed with Fenske rings. Refractive index measurements were used to control the purity of the distilled product. The pure quinoline from the column was collected under a natural gas atmosphere to isolate it from oxygen and was then stored at -20°C to hinder oxidation.

The feed stock was prepared by mixing appropriate amounts of quinoline and Peneteck to obtain the desired concentration of nitrogen. Fifty liters of feed stock containing approximately 1% N by weight were mixed up and stored in a glass container under a natural gas atmosphere. Most of the runs were made with this feed stock so enough was made at once to insure constant feed composition and characteristics. The feed stock was then simply siphoned from the container into the feed reservoir immediately preceding each run. The feed stock for the few runs made at other nitrogen levels was prepared immediately prior to each run.

Catalyst and Catalyst Supports: The shale oil work done at Montana State College (28) evaluated a number of commercially available catalysts. One of the better of these, a cobalt-molybdate catalyst manufactured by Peter Spence and Sons, Ltd., was chosen for our work. It was in the form

of 1/8-in. pellets and contained 2.5% CoO and 14.0% MoO_3.

The catalyst supports, used above and below the catalyst bed in the reactor, were 1/8-in. alundum pellets obtained from the Norton Abrasive Company.

Hydrogen Treat Gas: The hydrogen treat gas was supplied by HR Oxygen Supply, Billings, Montana. To remove trace quantities of oxygen, the hydrogen was first passed through a "Deoxo" unit. This unit contained a palladium catalyst which removed the oxygen by catalytically combining it with hydrogen to form water. The water was then removed by passing the hydrogen through a tube packed with "Drierite".

C. Equipment

Flow Diagram: A schematic flow diagram of the catalytic hydrogenation unit is shown in Figure 1. The reactor is operated as a fixed-bed, continuous-flow integral reactor. Feed stock from the oil feed reservoir is pumped to the inlet of a radiant preheater where it joins hydrogen which has been deoxygenated, dried, filtered, and metered from the hydrogen feed cylinder. Together, they pass through the preheater, enter the top of the reactor, and then travel downward through the preheat, catalyst, and after-heat sections. The vapors are then condensed, the liquid product being collected in a receiver at atmospheric pressure while the gaseous products are acid scrubbed and vented to the atmosphere.

Specifications: The reactor was made from a 30-in. length of nominal 1-in. OD, seamless, schedule 80, type 18-8 stainless steel pipe. It was equipped with a flanged union at each end to permit easy access. The reactor was covered with a layer of asbestos tape and then wrapped with five ceramic-beaded nichrome heating coils. A 2-in. layer of 85% magnesia insulation was placed over these heating coils.

A length of 3/16-in. OD stainless steel tubing, brazed shut at the lower end, extended through the middle of the reactor and served as a thermowell. In it were placed five iron-constantan thermocouples to measure temperatures at various positions in the reactor. The locations of the heating coils, thermocouples, and catalyst bed are shown in Figure 2.

The radiant preheater was constructed from a 3-in. x 11-in. stainless steel cylinder, closed on both ends. The cylinder was wrapped with asbestos tape, wound with a nichrome heating coil, and covered with a 2-in. layer of magnesia insulation. A 6-ft. length of 1/8-in. OD stainless steel tubing was coiled and placed in the cylinder. The oil and hydrogen passed through this coil before entering the reactor.

Accessory equipment which was also utilized in the hydrogenation unit is as follows: A Hills-McCanna high pressure proportioning pump with a 1/4-in. piston; two Brooks armored rotometers with 3/32-in. balls; one 220 volt Powerstat and five 110 volt Powerstats; an air-to-close, 1/2-in., Type No. 107-1, Mason-Neilan diaphragm valve; a reverse-acting, Type 4100 UR, Fisher-Wizard pressure controller; an 8-in. Jerguson sight glass; a

1000 ml glass oil reservoir with a 50 ml burette attached through a side arm; a Leeds & Northrup 18-point indicating potentiometer; two Marshall 2000 psi gauges; a Baker Deoxo Purifier, Model D; and two Matheson hydrogen regulators. Schedule 80 black-iron piping and Type 304 SS, 1/8-in. OD tubing were used throughout. Hoke #321 blunt-spindle valves were used for on-off control and Hoke 20 turn-to-open needle valves were used for metering. A 1500 psi rupture disk was placed in the reactor system as a safety precaution.

Toward the end of the investigation, the Mason-Neilan diaphragm valve, the Fisher-Wizard pressure controller, and the sight glass were all replaced by a Grove back pressure regulator. This regulator facilitated easier pressure control while allowing less liquid hold-up in the system.

D. Operating Procedures

Reactor Preparation: The reactor was charged by inverting the reactor tube, pouring catalyst supports to a predetermined level, charging the desired amount of catalyst, and filling the remainder of the tube with catalyst supports. When less than 100 gm of catalyst were used, enough catalyst supports were mixed with the catalyst so that the length of the catalyst bed was always the same. At 3 to 4-in. intervals of material charged, the reactor tube was tapped sharply with a hammer until there was no further tendency for the filler materials to settle. This was done to insure even packing and correct positioning of the catalyst bed. A stainless steel screen was fitted into place at the bottom of the reactor to keep the reactor contents in position. The reactor was then

coupled in its proper position in the unit; the oil and gas feed line, the thermocouple leads, and the Powerstat cords were connected to the reactor. After allowing hydrogen to flow through the reactor for an hour, the unit was pressurized and tested for leaks. It was then ready for a run.

Reactor Operation: In preparation for a run, the reactor was heated overnight under a hydrogen atmosphere. The feed pump was started when the desired operating temperature was reached and remained relatively constant. By adjusting the stroke of the piston in the feed pump, the space velocity was set to the desired value by measuring the volumetric oil feed rate. Hydrogen was metered through a rotometer and the flow rate adjusted with a needle valve. Temperatures throughout the reactor were measured with thermocouples and the Powerstats adjusted accordingly to maintain the desired temperature. By occasionally moving the thermocouples up and down in the thermowell, a complete temperature profile of the reactor was obtained to ensure the maintenance of isothermal conditions within the catalyst bed. A pressure controller and regulator valve were used to maintain the desired reactor pressure. The processed oil was collected in a sight glass and drained off steadily into a receiver. Late in the investigation, the pressure controller, regulator valve, and sight glass were replaced by a simple back-pressure regulator which functioned more satisfactorily.

Sampling: Benson (4) found in his investigations of shale oil that the conversion of nitrogen changed sharply during the first four hours of a run. It rose to a maximum, decreased sharply, and then leveled off to a reasonably constant value. This characteristic was attributed to an initial change in catalyst activity and was also encountered with quinoline system. Figure 3 shows this behavior for one of the runs which was conducted for 28 hours. From the figure it is apparent that a run must progress for six to eight hours before constant conversion is obtained. For this reason, sampling began only after temperatures remained constant and the run had progressed at least eight hours. Three successive samples were then taken, each consisting of a one-hour composite product of the run. Each sample was analyzed and the conversions checked against each other to ensure complete line-out.

E. Analytical Procedures

The nitrogen content of each sample was determined by the standard Kjeldahl method (24, 26). Duplicate determinations on the samples were averaged and the conversions obtained during each run were calculated from these values and the initial nitrogen concentration of the feed stock.

Some of the samples were further analyzed with a vapor-phase chromatography unit to determine the qualitative and quantitative distribution of reaction products and intermediates. This was accomplished with an Aerograph Model A-110-C gas chromatograph in conjunction with a Brown-Honeywell Model 143X57 1-mv recorder. A number of different columns

and column temperatures were used in this work.

Several fractionations of product were carried out on composite run samples to correlate product distribution with boiling point. The product fractions obtained were then subjected to chromatograph analysis and a few of them analyzed with a recording infra-red spectrophotometer.

IV. METHODS OF DATA ANALYSIS

A. Empirical Rate Equation

The rate of a reaction, also termed its velocity or speed, may be expressed in terms of the concentration of any of the substances which are reacting or of any product of the reaction. It is defined as the rate of decrease of the concentration of a reactant, or as the rate of increase of concentration of a product (25). Thus, if a reactant is chosen as the basis, having a concentration C at any time t, the rate is -dC/dt. Furthermore, the law of mass action states that the rate of a chemical reaction is proportional to the product of the "active masses" of the reactants involved. This law was first obtained experimentally by Guldberg and Waage in 1864 and subsequently derived from the theory of molecular collisions in gases and liquids (43). Since the activity of a substance in a mixture is frequently difficult to obtain, concentrations are usually used to replace the active mass terms. For example, in the reaction

$$A + B \longrightarrow R + S$$

we can express the rate as

$$r = -\frac{dC_A}{dt} = kC_A^a C_B^b$$

where r is the rate, C_A and C_B are the concentrations of the respective reactants A and B, a, b, and k are constants.

The constant k in the above equation is termed the "specific reaction rate constant", or simply the "rate constant". In general, its units

depend upon those employed for the concentration and upon the order of reaction. The order of reaction is defined as the sum of the exponents a and b. Reaction orders may have values of 0, 1, 2, 3, or some fractional value (9). This derivation of the rate equation based upon the law of mass action is theoretically valid only for homogeneous systems. However, it has been found that data from heterogeneous systems can also be correlated quite well in many cases. This is particularly true when one of the reactants is present in large excess (20).

In a heterogeneous catalytic reaction, a factor must also be included in the rate equation to account for the preparation, composition, and physical properties of the catalyst. Thus, for the overall reaction of

$$\text{Quinoline} + \text{Hydrogen} \longrightarrow \text{Hydrocarbons} + \text{Ammonia}$$

the rate could be expressed as

$$r = -\frac{dC_Q}{dt} = k_1 z C_Q^q C_H^h$$

where k is the rate constant, z is the catalyst factor, and C_Q and C_H are the concentrations of quinoline and hydrogen, respectively. This is, of course, assuming constant temperature and pressure.

If a large excess of hydrogen is used, as was the case in this study, the amount used up in the reaction is negligible and the hydrogen concentration remains essentially constant. Since the catalyst factor z is also constant for a given catalyst, both of these terms may be included in the rate constant. Furthermore, it is advisable to use the concentration of nitrogen rather than the concentration of quinoline in defining

the rate. Doing this, the rate equation becomes

$$r = -\frac{dC_N}{dt} = k_2 C_N^n$$

where C_N is the concentration of nitrogen.

For purposes of data evaluation, the equation is put into a better form by letting A be the original amount of nitrogen present and x be the amount converted. The A-x is the amount of nigrogen left, or C_N. The equation then becomes

$$r = \frac{dx}{dt} = k_2(A-x)^n \qquad (1)$$

Separating the variables and integrating from x = 0 to x = x and t = 0 to t = t gives

$$\int_0^x \frac{dx}{(A-x)^n} = k_2 t$$

Since the actual contact time t is virtually impossible to calculate, it has been found convenient to introduce a new variable, space velocity or S_v. Space velocity is defined as the volume or weight of reacting mass per unit volume or weight of catalyst per unit time. In some cases unit volume of reactor is used in place of unit volume of catalyst (9). For this work we shall define space velocity as grams of oil per gram of catalyst per hour. Since the specific units are then reciprocal time, we may use $1/S_v$ in place of time in the rate equation, thus obtaining

$$\int_0^x \frac{dx}{(A-x)^n} = \frac{k_e}{S_v} \qquad (2)$$

B. Order of Reaction

The order of reaction is then n, the exponent of the A-x term of Equation 2. However, this is termed a "pseudo order" since it is actually a ficticious order obtained by letting one of the reactants be in large excess of that required for complete conversion (20).

The most common method for evaluating n is to assume different orders of reaction until one is found which agrees with the data. For example, if the reaction is first order, n is equal to one, and

$$\int_0^x \frac{dx}{A-x} = \frac{k_e}{S_v}$$

which integrates to give

$$\ln \frac{A}{A-x} = \frac{k_e}{S_v} \qquad (3)$$

A plot of ln A/A-x vs. $1/S_v$ would then yield a straight line with a slope of k_e and an intercept of zero.

For a second order reaction, n has a value of two and the rate equation becomes

$$\int_0^x \frac{dx}{(A-x)^2} = \frac{k_e}{S_v}$$

Integrating this equation gives

$$\frac{1}{A-x} - \frac{1}{A} = \frac{k_e}{S_v} \qquad (4)$$

In this case, a plot of $1/A-x$ vs. $1/S_v$ would give a straight line having a slope of k_e and an intercept of $1/A$.

By making such plots, the order of this reaction was determined at three different pressures. Quite often, visual inspection of the plot is sufficient to discard or accept the assumed order. Where there is question of results, statistics can be helpful in evaluating the "goodness of fit" of the data. In any event, the data points should not show a definite upward or downward trend (9).

C. Energy of Activation

The effect of temperature on a chemical reaction, the change of the reaction rate constant, is usually expressed by means of the Arrhenius equation. Although Arrhenius developed his concept in 1889, modern kinetic data agree with it remarkably well (36). The Arrhenius equation is based upon the variation of the equilibrium constant with temperature, i.e., the van't Hoff equation, and is expressed as

$$k = se^{-E_a/RT} \tag{5a}$$

or

$$\ln k = \frac{-E_a}{RT} + \ln s \tag{5b}$$

where k is the reaction rate constant, R is the universal gas constant, T is the absolute temperature, s is a constant called the "frequency factor", and E_a is termed the energy of activation.

The so-called activation energy was interpreted by Arrhenius as the excess over the average energy that the reactants must possess in order for the reaction to occur (36). The overall reaction could then be looked upon as occuring by the following two-step process:

Reactants $\longrightarrow$ Activated Reactants $\longrightarrow$ Products

Arrhenius regarded the activation energy as a "heat" term and compared it to the heat of reaction. Eyring has since shown that it is really a free energy term and not an enthalpy term as had been previously supposed (16).

According to the equation, plots of ln k vs. 1/T will give a straight line with a slope of $-E_a/R$ and an intercept of ln s. These plots were made and the corresponding activation energies obtained.

D. Reaction Mechanism

Theory: When a chemical reaction takes place without the aid of a catalyst, the only steps involved are chemical ones. The case is different in catalysis, however; here, the steps that constitute the mechanism are both physical and chemical. The reaction on a solid catalyst may be divided into the following steps (9):

1. Diffusion of the reactant molecules to the surface of the catalyst.
2. Diffusion into the pores of the catalyst.
3. Adsorption of the reactant onto the catalyst.
4. The actual chemical reaction or series of reactions which take place in the adsorbed phase on the catalyst.

5. Desorption of the product molecules.
6. Diffusion of the products to the exterior of the catalyst pellet.
7. Diffusion from the pellet to the main gas stream.

Steps 1, 2, 6, and 7 are definitely physical steps and the rates of these steps are determined by the laws of diffusion. Step 4 is a chemical step and describes the actual transformation of reactant molecules to product molecules. Steps 3 and 5 lie on the borderline between physical and chemical. If the adsorption takes place by chemisorption, these are classified as chemical steps.

Chemisorption refers to adsorption where there is actual chemical combination between the adsorbate molecules and the catalyst. Taylor first proposed that reactions which are catalyzed by solids actually occur on the surface of the solids at points of high chemical activity which are called "active centers" (40). The exact nature of an active center and the conditions which must be fulfilled in order that a point on the surface becomes [illegible] active remains the subject of much speculation. There is evidence that the interatomic spacing of the solid structure is important as well as the chemical constitution and lattice structure. The belief that definite electron bonds are involved, corresponding to the formation of a chemical compound between the adsorbate and the surface, is supported by the large enthalpy change accompanying adsorption (20). Regardless of the nature of active centers, their existence is the basis of the theories of chemisorption.

Since the seven steps listed above occur in series, it is possible for any one of them to control the over-all rate of the reaction. It is usually assumed that the rate of one of the steps is appreciably slower than that of the others; the over-all rate will then adjust itself to that of the slow step. This slow step is termed the "rate controlling step" and can be either a physical or a chemical one.

Diffusion Controlling: If any one of the physical steps is rate controlling, it is an indication that the catalyst is not being used to its fullest capacity. If step 1 or 7 is controlling, it means that either the reactant molecules can not be supplied to the catalyst or that the product can not be removed fast enough to keep up with the potential ability of the catalyst to cause the reaction to proceed. This occurs because the reactants and products must diffuse through a stagnant layer of gas that surrounds the catalyst pellet (9).

The effects of this film diffusion were checked by making a series of runs at constant space velocity but different linear velocities. This was accomplished by varying the feed rate and weight of catalyst simultaneously to give the same value of S_V. If the values of conversion for the different gas velocities coincide, the effect of diffusion is negligible; conversely, there is a diffusional effect if the conversions are different. This occurs because an increase in the gas velocity will lower the film resistance by sweeping away more of the stagnant gas layer, thereby increasing the rate of diffusion. If film diffusion is rate controlling, a subsequent increase in conversion takes place. The usual procedure

is then to redesign the reactor such that high enough gas velocities are obtained to minimize diffusional effects.

Even with a gas velocity large enough to keep the film resistance at a minimum, it is still possible that the catalyst is not used to its fullest capacity. This occurs when either step 2 or step 6 in controlling.

In most catalysts the outside surface area is negligible in comparison to the vast interior pore surface. In order for this interior surface to be used, the reactant molecules must diffuse into the pores and the products must diffuse out again. Thus, if this interior diffusion is controlling, use of a smaller catalyst will speed up the reaction (9). Runs were made using three different catalyst sizes to check for the effect of interior diffusion. These different size catalysts were prepared by simply crushing and screening the original 1/8-in. pellets of catalyst. A small enough catalyst particle to limit the effects of internal diffusion was then chosen for the balance of the study.

Chemical Step Controlling: After the effects of film and internal diffusion are minimized, it is possible to study the actual mechanism of the reaction. Here, the term mechanism shall refer to the various adsorption, reaction, and desorption steps which take place on the surface of the catalyst.

As will be shown later, the hydrogenation of quinoline actually proceeds through several intermediate compounds before the final products are obtained. The slowest of these reactions, as the case may be, will control the overall rate of reaction. This is subsequently shown to be the final

reaction: the addition of hydrogen to a primary amine, formed when the quinoline molecule is broken open, to yield the products of ammonia and propyl benzene. In the following analysis, it is this reaction which is discussed. This reaction can be expressed in an overall manner as:

$$A + H_2 \longrightarrow R + S \qquad (6)$$

where A refers to the forementioned amine, H_2 is molecular hydrogen, and R and S are the reaction products of ammonia and propyl benzene.

There are a number of mechanisms whereby this reaction could proceed. To determine the correct mechanism and controlling step, one must postulate the various ways the reaction could take place, writing down each step and and corresponding rate equations. The rate equations, assuming each successive step controlling, are then examined in light of the experimental data and any which do not agree with the data are rejected. The mechanism which cannot be rejected, or the one which fits best if there are several, is then chosen as the correct mechanism.

The five most plausible mechanisms whereby this reaction could proceed are as follows:

I. Reaction between molecularly adsorbed hydrogen and adsorbed amine.

II. Reaction between atomically adsorbed hydrogen and adsorbed amine.

III. Reaction between molecularly adsorbed hydrogen and amine in the gas phase.

IV. Reaction between molecularly adsorbed hydrogen and amine in the gas phase.

V. Reaction between hydrogen in the gas phase and adsorbed amine.

The postulated steps for each mechanism and their corresponding rate equations are shown in Table XII.

The development of the equations for one of the steps controlling for Mechanism I will now be considered. Suppose that the reaction between molecularly adsorbed hydrogen and adsorbed amine takes place by the following steps:

1. A molecule of A is adsorbed upon an active center of the catalyst.
2. A molecule of hydrogen is adsorbed upon an adjacent center of the catalyst.
3. The adsorbed molecule of A then reacts with the adsorbed molecule of hydrogen to form the products R and S adsorbed on active sites.
4. The molecule of R is desorbed from the active site.
5. The molecule of S is desorbed from the active site.

Using the symbol, v, to designate a vacant active center, we can write the chemical equations for these steps as:

1. $A + v \rightleftarrows Av$ $\qquad K_1 = C_A/P_A C_v$ (7)

2. $H_2 + v \rightleftarrows H_2v$ $\qquad K_2 = C_{H_2}/P_{H_2} C_v$ (8)

3. $Av + H_2v \rightleftarrows Rv + Sv$ $\qquad K_3 = C_R C_S / C_A C_{H_2}$ (9)

4. $Rv \rightleftarrows R + v$ $\qquad K_4 = P_R C_v / C_R$ (10)

5. $Sv \rightleftarrows S + v$ $\qquad K_5 = P_S C_v / C_S$ (11)

In these equations K_1, K_2, K_3, K_4, and K_5 represent the equilibrium constants for the individual steps; C_A, C_{H_2}, C_R, and C_S are the concentrations of the adsorbed gases; and C_v is the concentration of vacant active centers. If any one of the above steps is slower than the others, it will be the rate controlling step. The final form of the rate equation will depend upon which of the steps is the slow one.

The derivation of the rate equations is based upon the following assumptions:

1. The resistance to diffusion is negligible so that only a chemical step can control the reaction. Furthermore, this resistance is so slight that the partial pressure at the interface can be replaced by the partial pressure in the bulk of the gas stream.
2. The adsorption terms are all chemisorption and react according to the law of mass action.
3. Only one of the reaction steps is rate controlling and there is no shift of the controlling step during the reaction.

4. The rate equation for the rate controlling step can be written as a simple order reaction.

5. The specific rate constants and equilibrium adsorption constants are independent of total pressure.

As an example of the derivation, suppose that step 1, the adsorption of the amine, is the slow one. The rate of step 1 is then equal to the overall rate since the rest of the steps are at equilibrium. Assuming this step to be of simple order, the rate equation is

$$r = k_1 P_A C_V - k_1' C_A \tag{12}$$

where k_1 and k_1' may be regarded as forward and reverse constants. At equilibrium, the rate is zero and

$$C_A / P_A C_V = k_1 / k_1' = K_1$$

Therefore we can write

$$k_1' = k_1 / K_1$$

and Equation 12 reduces to

$$r = k_1 (P_A C_V - C_A / K_1) \tag{13}$$

However, this equation cannot be used as it stands since it contains the terms C_A and C_V, variables that cannot be measured. These quantities must be expressed in terms of variables that can be measured--the partial pressures of A, B, R, or S.

Since step 1 is the rate controlling step, it is not in equilibrium and the equation $K_1 = C_A/P_A C_V$ cannot be used to evaluate C_A. However, steps 2, 3, 4, and 5 are at equilibrium and the corresponding equilibrium equations may be used. From Equations 8, 10, and 11:

$$C_{H_2} = K_2 P_{H_2} C_V$$

$$C_R = P_R C_V / K_4$$

$$C_S = P_S C_V / K_5$$

Substituting these values into Equation 9 gives:

$$C_A = P_R P_S C_V / K_2 K_3 K_4 K_5 P_{H_2}$$

This value of C_A can now be put into Equation 13 to give:

$$r = k_1 (P_A C_V - P_R P_S C_V / K_1 K_2 K_3 K_4 K_5 P_{H_2})$$

Since steps 1 and 5 add up to the overall reaction, the product $K_1 K_2 K_3 K_4 K_5$ must be equal to the overall equilibrium constant, K. Substituting in this value of K and factoring out C_V:

$$r = k_1 C_V (P_A - P_R P_S / K P_{H_2}) \qquad (14)$$

This leaves C_V as the only variable that cannot be determined experimentally. The total number of active centers, which is independent of conversion, is defined as V. Then we can write

$$V = C_V + C_A + C_{H_2} + C_R + C_S$$

Substitution of the values for C_A, C_{H_2}, C_R, and C_S gives:

$$V = C_V + P_R P_S C_V / K_2 K_3 K_4 K_5 P_{H_2} + K_2 P_{H_2} C_V + P_R C_V / K_4 + P_S C_V / K_5$$

Solving for C_V gives:

$$C_V = \frac{V}{1 + P_R P_S / K_2 K_3 K_4 K_5 P_{H_2} + K_2 P_{H_2} + P_R / K_4 + P_S / K_5}$$

With the substitution of this value of C_V, Equation 14 becomes:

$$r = \frac{k_1 V (P_A - P_R P_S / K P_{H_2})}{1 + P_R P_S / K_2 K_3 K_4 K_5 P_{H_2} + K_2 P_{H_2} + P_R / K_4 + P_S / K_5}$$

or

$$r = \frac{k (P_A - P_R P_S / K P_{H_2})}{1 + K_A P_R P_S / P_{H_2} + K_4 P_{H_2} + K_R P_R + K_S P_S}$$

where

$k = k_1 V$; $K_A = 1/K_2 K_3 K_4 K_5$; $K_H = K_2$; $K_R = 1/K_4$ and $K_S = 1/K_5$.

Also, if an inert gas is present, it must be taken into account if it is adsorbed (43). Once the flow process is in operation, the catalyst will become saturated with respect to the inert component and the composition of the inerts will not change. Assume that the carrier oil in this case is adsorbed according to the reaction:

$$I + v \rightleftarrows Iv \qquad K_I = C_I / P_I C_V \qquad (15)$$

where I refers to the inert oil. This will simply add another term to the denominator of the rate equation which then becomes:

$$r = \frac{k(P_A - P_R P_S / K P_{H_2})}{1 + K_A P_R P_S / P_{H_2} + K_H P_{H_2} + K_R P_R + K_S P_S + K_I P_I} \qquad (16)$$

Since this rate equation contains five variables (P_A, P_{H_2}, P_R, P_S and P_I), it is still too unwieldy for the purpose of picking the correct mechanism. Several authors (9, 21, 43) suggest the use of initial rate data rather than finite rate data for this purpose. At the initial point where x equals zero, P_R and P_S also are zero and the rate equation becomes:

$$r_o = \frac{k P_{A_o}}{1 + K_H P_{H_2} + K_I P_I} \qquad (17)$$

where the subscript zeros refer to the initial rate and partial pressures. Table XIII shows the corresponding initial rate equations assuming each step controlling in each of the mechanisms.

Replacing the partial pressures of each component by the product of their mole fractions times the total pressure, the above equation becomes:

$$r_o = \frac{k y_{A_o} \pi}{1 + K_H y_{H_o} \pi + K_I y_I \pi} \qquad (18)$$

where the y's represent the respective mole fractions and π is the total pressure. The initial rate can then be studied as a function of total pressure or initial composition, in each case holding the other constant.

For example, at constant initial composition, dividing the above equation through by $k y_A$ gives:

$$r_o = \frac{\pi}{a + b\,\pi} \qquad (19)$$

where $a = 1/ky_{A_o}$ and $b = (K_H y_{H_o} + K_I y_I)/ky_{A_o}$. This form of the initial rate equation for each step controlling is shown in Table XIV and the corresponding curves are shown in Figure 12. Furthermore, a and b are restricted to be positive constants in each of the equations. Comparison of a plot of experimental r_o vs. π (or a function of r_o vs. π) to the curves defined by the derived equations serves as a basis for rejection of unacceptable mechanisms. This was done and a majority of the postulated mechanisms were rejected.

The remaining ones were studied by holding the pressure and y_{H_o} constant and varying y_{A_o} and y_I. Substituting $y_I = 1 - y_{A_o} - y_{H_o}$ and dividing Equation 24 through by $k\,\pi$ gives:

$$r_o = \frac{y_{A_o}}{1/k\,\pi\,[1 + K_H y_{H_o}\,\pi + K_I(1-y_{H_o})\,\pi\,] - 1/k\,K_I y_A} \qquad (20)$$

or

$$r_o = \frac{y_{A_o}}{a' + b' y_{A_o}}$$

where a' and b' refer to the appropriate constants. In this case, the constant b' may or may not be positive, depending upon the controlling step. Plots of functions of r_o vs. y_{A_o} then served to eliminate all but one of the remaining assumed mechanisms.

The rate of reaction is defined as dx/dt (Equation 1), and can be evaluated in several ways. From a plot of x vs. t, the slope at the

origin, where t is zero, corresponds to the initial rate. However, finding rates by slope measurement is not too satisfactory in general because of the inherent inaccuracies in drawing the curve and constructing tangents. A better method is to find a satisfactory empirical correlation which expresses x as a function of t. Differentiation of this equation with respect to t then gives an expression for the rate of reaction which can be evaluated at any desired t. At t equal zero, the initial rate is obtained. This was the method employed in this study. Finding the empirical correlation was discussed under the "order of reaction" concept.

V DISCUSSION AND EXPERIMENTAL RESULTS

A. Exploratory Runs:

A number of runs were made at various processing conditions to establish the general range of operating conditions previously mentioned. Since these runs merely served as a guide, their analysis is not included here. Of note are Runs 1-6 made with pure Peneteck to establish the effect of temperature on breakdown of the Peneteck. These runs were made at 25 degree intervals from 700°F to 825°F. Chromatograph analysis of the processed oil indicated negligible effect under 775°F (413°C) at the relatively severe operating conditions of 1000 psi and S_V of 1. Above 775°F the breakdown increased sharply until at 825°F (441°C) about 20-25 percent of the Peneteck was affected. Hence, it was decided to carry out the majority of this study at 725°F (385°C), well below the temperature of any Peneteck breakdown.

B. Conversion-Time Study:

Run 7 was carried out for 28 hours to determine the length of run necessary to insure complete lineout. Results of this run are shown in Table V and conversion vs. hours on stream is plotted in Figure 3. It is seen that the conversion drops sharply during the first few hours of operation and then levels off to a reasonably constant value after eight hours on stream. This sharp change in conversion is attributed to the initial adsorption of the oil upon the catalyst until it is completely saturated and equilibrium is established. The slight decline in conversion thereafter occurs due to a decrease in catalyst activity,

probably caused by a blocking of active sites due to carbon formation.

Benson (4) found that this line-out time was longest at low pressures and low space velocities. Since the conditions of this run were essentially at the lowest pressure and space velocity used in the study (250 psig and 1/2 g/g hr), it was assumed that all runs would be at equilibrium after eight hours. Therefore, sampling began after eight hours on-stream time and three successive hour samples were collected. Total nitrogen content was determined on each sample and the values compared to check on line-out.

C. Tests for Diffusion:

The effects of film diffusion were checked with Runs 8-11. These runs were made at different linear velocities but with a constant space velocity obtained by varying the feed rate and amount of catalyst simultaneously. Feed rates varied approximately from 0.5 to 2.5 g/min and amount of catalyst from 15 to 75 grams. The results of the runs are shown in Table VI and conversion vs. grams of catalyst is plotted in Figure 4.

Although some deviation in the conversions is noted, there is no general trend. If film diffusion controlled the reaction, a higher conversion would result when larger amounts of catalyst were used. Therefore, it is concluded that the effect of film diffusion is not significant when using more than 15 grams of catalyst and a feed rate greater than 0.5 g/min. Furthermore, since these runs were made at 1000 psig, negligible diffusional effects are expected on operation at

low pressures since at constant space velocity a correspondingly higher linear velocity will result when the pressure is decreased. All subsequent runs were then made to conform to these limits.

Internal diffusion was checked with Runs 12-14. In these runs, the catalyst particle size was changed while all other processing conditions remained constant. Table VII shows the data for these runs and Figure 5 is a plot of conversion vs. catalyst size.

To prepare the different size catalysts, the original 1/8-in. pellets were crushed with a mortar and pestle and then sized with a set of Taylor screens. The 10-16 and 16-35 mesh fractions were collected and each used in a separate run in addition to a run with the 1/8-in. pellets. From the results it is apparent that internal diffusion is not a significant factor.

D. Empirical Rate Equation:

A series of runs at each of three different pressures and over a range of varying space velocities were made to determine an empirical rate equation. This equation was then used to calculate initial rates of reaction which were needed for subsequent correlations. The three pressures used were 250, 500, and 1000 psig, and the space velocity was varied from 1/3 to 10 g/g hr. The data from the runs are tabulated in Table VIII and conversion vs. space velocity with pressure as a parameter is plotted in Figure 6.

The molecularity of the reaction suggests a pseudo first order reaction when a large excess of hydrogen is used. Therefore, correspond-

ing to Equation 3, plots of ln A/A-x vs. $1/S_V$ were made and are shown in Figure 7. The method of least squares was used to obtain the best straight line representing the data. It is seen that the assumption of first order kinetics appears to correlate the data very well. There is some scatter in the points, undoubtedly due to experimental error, but no significant upward or downward trend of the points from the straight line.

For comparison, the same data are plotted in Figure 8 assuming a second order reaction. In this case, plots were made of 1/A-x vs. $1/S_V$, corresponding to Equation 4. Inspection of the plots shows a definite upward trend in the data points, particularly at the higher pressures.

Since the assumption of a pseudo first order reaction fits the data quite well, it was decided to use the corresponding equation as an empirical rate equation. The slope of the resulting straight line is then the empirical reaction rate constant, k_e, of Equation 3. The calculated values are 0.0944, 0.2675, and 0.7502 hr^{-1} at the three pressures of 250, 500, and 1000 psig, respectively.

E. Energy of Activation:

The energy of activation for the reaction studied was determined from the Arrhenius Equation (Equation 5-b), relating the change of reaction rate constant to temperature. To do this, runs were made at 750, 775, and 800°F for each of the three pressures. Using the previous

data at 725°F then gave four data points at each pressure.

Evaluation of the activation energy is accomplished by plotting $\ln k_e$ vs. $1/T$. Since only one run was made at each of the higher corresponding temperatures and pressures, it was impossible to check this data for order of reaction. However, assuming that the pseudo first order reaction still holds, the reaction rate constants can be calculated from Equation 3. All the runs in this series were made at a space velocity of 1.0, so Equation 3 reduces to

$$k_e = \ln A/A-x$$

The rate constants calculated from this equation, along with associated data, are tabulated in Table IX and $\ln k_e$ vs. $1/T$ is plotted in Figure 9.

From the Arrhenius Theory, this plot should be a straight line. It is seen that the data at 250 psig fits quite well but at the other two pressures the point at the highest temperature of 800°F is considerably off. This is most likely caused by a change in reaction mechanism; or at least the addition of a competing reaction, since it had been noticed previously that considerable breakdown of the Peneteck occurred above 800°F. The point at 1000 psig is furthermore unsatisfactory from an analytical standpoint. The conversion at those conditions was so high that a slight error in conversion changes the ratio $A/A-x$, and subsequently k_e, by a considerable amount. For this reason, these two points were neglected when fitting the best straight line at each pressure.

The slope of the resulting straight line is then $-E_a/R$. From the slopes, the corresponding activation energies were calculated to be 33.7, 30.4, and 23.6 K cal/mole at 250, 500, and 1000 psig, respectively. The exact reason for the change of activation energy with pressure is not known. However, this seems perfectly reasonable since the activation energy can be thought of as a measure of the difficulty in causing the reaction to take place. It is frequently pictured as an energy barrier which the reactant molecules must overcome before reaction occurs. Activation energy vs. pressure is plotted in Figure 10 and it is interesting to note that the plot shows a linear relationship.

F. Reaction Rates:

The pseudo first order reaction equation, Equation 3, can be written as:

$$r = dx/dt = k_e(A-x) \qquad (3\text{-a})$$

or

$$\ln A/A-x = k_e/S_V \qquad (3\text{-b})$$

in integrated form.

This equation can be written in exponential form as:

$$A/A-x = e^{-k_e/S_V}$$

or

$$A-x = A_e^{-k_e/S_V}$$

Substituting this value of A-x into Equation 3-a, the empirical rate equation becomes:

$$r = k_e A e^{-k_e/S_V} \qquad (3\text{-}c)$$

Thus, using the previously calculated values of k_e, the rate of reaction can be found at any desired value of S_V.

At time zero (infinite S_V), Equation 3 reduces to:

$$r_o = k_e A \qquad (21)$$

and the initial rate of reaction can be calculated. Using this equation, the initial rates were determined for each previous run or series of runs except those at 800°F, which did not appear reliable. The values obtained are tabulated in Table X. In addition, a series of runs at 500 psig and 725°F were made with varying initial nitrogen content, their initial rates calculated, and the results tabulated in Table XI. These initial rates are then used in determining the reaction mechanism. The data of Table X are plotted as r_o vs. π in Figure 11.

G. Reaction Mechanism:

The five postulated mechanisms and their corresponding twenty steps are shown in Table XII. The rate equations obtained by assuming each successive step rate controlling with the other steps at equilibrium are listed in Table XIII. With constant initial composition, total pressure being the independent variable, these equations reduce to those shown in Table XIV.

These equations were first graphed as r_o vs. π in Figure 12 and compared to the plots of experimental data of Figure 11. Visual in-

spection is sufficient to reject most of the possible rate controlling steps. The experimental plots show a concave upward curve over the pressure range studied. Thus, the graph of any initial rate equation was rejected if it did not show a concave upward curve, at least in the initial part of the graph. On this basis, all steps except (1), (s), (c), (o), and (h) were rejected.

The data at variable initial nitrogen content (constant pressure) were then used to differentiate between the five remaining steps. The equations for these steps can be simplified at constant pressure in the manner previously shown to give:

$$\text{Steps (1), (s), (g):} \quad y_A y_H / r_o = a'' + b'' y_A \tag{22-a}$$

$$\text{Steps (c), (o):} \quad \sqrt{y_A y_H / r_o = a'' + b'' y_A} \tag{22-b}$$

$$\text{Step (h):} \quad \sqrt[3]{y_A y_H / r_o = a'' + b'' y_A} \tag{22-c}$$

Thus, plots of the left side of each of the above equations vs. y_A will test the remaining steps. Any step which is acceptable will yield a straight line.

The data for these plots are shown in Table XV. In Figure 13 are plotted $y_A y_H / r_o$ vs. y_A and $(y_A y_H / r_o)^{1/3}$ vs. y_A. Both resulting plots show a definite curve so the corresponding mechanism steps are rejected. On the other hand, the graph of $(y_A y_H / r_o)^{1/2}$ vs. y_A in Figure 14 appears to fit a straight line quite well. Thus, all steps except (c) and (o) are rejected as rate controlling steps.

However, closer inspection of Equation 22-b will also eliminate step (o). In the derivation of this equation, before complete simplification, it was actually:

$$\text{Step (o):} \qquad \sqrt{y_A y_H / r_o} = a'' - c y_A / \pi \qquad (23\text{-a})$$

$$\text{Step (c):} \qquad \sqrt{y_A y_H / r_o} = a'' + (c-d) y_A / \pi \qquad (23\text{-b})$$

Since c and d are restricted to be positive constants, Equation 23-a will give a straight line of negative slope and Equation 23-b will give a straight line of either positive or negative slope depending on the magnitudes of c and d. The experimental data definitely show a positive slope, so step (o) is rejected on that basis.

The validity of step (c) as the rate controlling step can be further checked by rearranging the initial rate equation at constant feed composition to give:

$$\pi^2 / r_o = (a + b\pi)^2$$

or

$$\sqrt{\pi^2 / r_o} = a + b\pi \qquad (24)$$

Again, a straight line of positive slope should result when plotting $(\pi^2/r_o)^{1/2}$ vs. π. The data for these plots are shown in Table X. From Figure 15 it is seen that the data fit a straight line very well at 750°F and 775°F while some scatter of points occurs at 725°F. In general, the data agree well enough so that step (c) again cannot be rejected.

This, then, leaves step (c) as the only postulated rate controlling step that passes all tests and cannot be rejected on the basis of these experimental data. It is therefore accepted that the reaction takes place according to Mechanism I, the dual-site surface reaction between molecularly adsorbed hydrogen and adsorbed amine, with the surface reaction itself controlling the rate of reaction.

It should be emphasized at this point that the accepted mechanism is not necessarily the only acceptable mechanism. Simply because the experimental data fit the accepted mechanism over the range of variables studied does not guarantee a unique solution. It is quite possible that a new sequence of steps could be postulated that would fit the data just as well.

The final form of the rate equation is then accepted as:

$$r = \frac{kK_1K_2\left[P_AP_{H_2} - P_RP_S/K\right]}{\left(1 + K_1P_A + K_2P_{H_2} + P_R/K_4 + P_S/K_5 + P_I/K_6\right)^2}$$

where k is the overall reaction velocity constant, K refers to the particular equilibrium constants for the adsorption-desorption steps, and P represents the partial pressure of the components. The equilibrium constants and the velocity constants are all exponential functions of temperature.

Evaluation of these constants was not accomplished in this study. To do this, more data would be required at various combinations of temperature, pressure, reactant ratios and conversions. Finite rate data rather than initial rate would be necessary for this purpose.

H. Identification of Reaction Products and Intermediates:

The identification of the reaction products and intermediates was accomplished by using the method of vapor-phase chromatography, supplanted with infra-red spectrophotometry, fractionation with correlation of boiling points and refractive indices, and chemical tests.

A vapor-phase chromatograph works essentially as a highly efficient distillation column. In addition, it allows the analysis of very small samples in a matter of minutes. In this work, samples in the range of one to five microliters were used and analysis was achieved in a maximum of 30 minutes. After injection, the sample is carried by a stream of helium into the packed column where it is selectively adsorbed on the substrate. The adsorption properties of each compound determine their respective retention times in the column. Selection of the proper column and operating conditions will completely resolve most compounds, even isomers in many cases.

The stream of gas emerging from the column passes through a sensing element which measures its thermal conductivity and compares it to a standard (helium). This change in thermal conductivity is shown on a continuous chart recorder as a series of peaks, one for each compound as it emerges from the column. Thus, the area under any peak will be a measure of the quantity of that particular compound. For a homologous series, the quantity of a compound as determined from the peak area will be accurate to within a few percent error. For a series of dissimilar compounds, a much greater error will result

because of different thermal conductivity characteristics. In this study, product distribution was calculated assuming constant thermal conductivity characteristics.

In order to study the reaction intermediates formed, it was necessary to use cetane as a carrier oil rather than Peneteck. From previous runs it was found that the Peneteck peaks covered up some of the intermediate peaks in chromatographic analysis. Thus, Runs 39, 40, and 41 were made with cetane under conditions which gave approximately 10, 54, and 96 percent conversion. The data for these runs are shown in Table XVI.

Figures 16, 17, and 18 are traces of the chromatograms of these runs. It is seen that there are some twenty or so peaks, each representing one or more compounds. The relative size of each peak depends upon the conversion of the particular run. The chromatograms read from right to left; those compounds emerging from the column first appear on the right side of the trace.

The peaks due to cetane and quinoline are easily established by making chromatograms of these compounds separately. Figure 19 is a trace of cetane and shows that peak 21, attenuated eight times, is cetane itself, while peaks 16, 19, 20, and 22 are due to impurities in the cetane. A chromatogram of the oil feed containing approximately 1.5 wt % N as quinoline is shown in Figure 20. From this figure it is apparent that peak 17 corresponds to the quinoline.

Figure 16 shows that at 10 percent conversion roughly half of the remaining nitrogen is in the compound represented by peak 18. At 54 percent conversion, Figure 17 shows that this peak as well as the quinoline peak has essentially disappeared. It was suspected that the reaction goes by first hydrogenating the nitrogen ring of quinoline to yield tetrahydroquinoline. Figure 21 is a trace of the oil feed to which had been added a small amount of tetrahydroquinoline. From this figure it is seen that the tetrahydroquinoline comes out of the column at almost the same time as one of the cetane impurities and completely covers peak 19. Thus, it is concluded that peak 18 represents tetrahydroquinoline, an intermediate in the reaction. The reaction therefore probably takes place by adding a hydrogen molecule to quinoline to form dihydroquinoline and then a second hydrogen molecule to this compound to form tetrahydroquinoline. Although no dihydroquinoline was identified, it seems reasonable that it would be formed first before the tetrahydroquinoline.

Whitmore (45) states that with metals and acids, quinoline hydrogenates to dihydroquinoline and this compound further readily adds a second hydrogen to form tetrahydroquinoline. It may well be that the addition of the second hydrogen goes so fast that only a very small amount of the dihydro compound is present at any time and whatever is there, is covered up by one of the other peaks.

At 54 percent conversion, Figure 17 shows peaks 12, 13, 14, and 15 to predominate and then essentially disappear at 96 percent con-

version as shown by Figure 18. These peaks are then further nitrogen-containing intermediates in the reaction. These compounds were identified by first fractionating a composite of excess product from several runs and continuously collecting small samples. The samples which contained a major portion of each of the intermediates, as indicated by chromatographic analysis, were then subjected to the VanSlyke nitrous acid test (44) to test for various amines. In each case, no reaction took place in the cold but reaction with evolution of nitrogen took place on subsequent warming. This showed the presence of primary aromatic amines which was further substantiated by analysis with an infra-red spectrophotometer. Refractive indices of the samples were about 1.55, in the general range of amines. Furthermore, the boiling points as indicated by the fractionation correspond to those of aniline and its methyl, ethyl, and propyl homologs. Chromatogram traces of aniline, o-methylaniline and o-ethylaniline showed these compounds to correspond to peaks 12, 13, and 14. No o-propylaniline was available for comparison but peak 15 undoubtedly represents this compound.

Thus, it is concluded that the third step in the hydrogenation involves opening up of the nitrogen ring of tetrahydroquinoline and addition of a third hydrogen molecule to form primarily o-propyl-aniline. Smaller amounts of aniline, o-methylaniline and o-ethyl-aniline are also formed. It was not determined whether these last three compounds occur as a result of cleavage of the ring in a different place or by splitting off part of the side chain of o-propyl-aniline. Small amounts could also occur from any isoquinoline impurity

present in the reactants. Quite likely, there is some contribution from each of the side reactions mentioned. At 10 percent conversion, the distribution of these intermediates as calculated from the area under the peaks is:

o-propylaniline:	71%
o-ethylaniline:	5%
o-methylaniline:	17%
aniline:	7%

At higher conversions the percentage of o-propylaniline is somewhat less and there is correspondingly more of the other three compounds. Chromatograms made from the runs at various temperatures and pressures seemed to show little change in this distribution.

The final reaction products are indicated by the cluster of peaks preceding peak 12. Better resolution of these compounds is obtained by operating the chromatograph at a lower temperature as shown in Figure 22. By the same method of comparing chromatograms of known compounds and checking boiling points and refractive indices, the reaction products were identified to be those listed on Figure 22. The distribution of the products of this particular run was calculated as:

cyclohexane	1.4%
benzene	1.1%
methylcyclohexane	1.4%
toluene	2.2%
ethylcyclohexane	3.0%
ethylbenzene	2.1%
iso-propylbenzene	60.8%
propylcyclohexane	6.4%
n-propylbenzene	17.7%
o-ethyltoluene	3.9%

Thus, the fourth step in the reaction is the addition of another hydrogen to the intermediate amines to split off ammonia and leave aromatic homologs as the reaction products. The main products are seen to be iso-propylbenzene and n-propylbenzene. In addition, small amounts of the aromatics are further hydrogenated to yield their corresponding alicyclic compounds.

Degree of conversion seemed to have little effect on this distribution. However, the pressure at which a run was carried out had a marked effect. Figure 23 shows chromatogram traces of runs made at three different pressures. The most noticeable effect appears to be the reduction in the amount of iso-propylbenzene produced at higher pressures. Close inspection of the traces will also reveal the corresponding apparent suppression of alicyclic formation.

Figure 24 is the chromatogram from a run made at 800°F. Here it is seen that there is a considerably greater portion of the lower aromatics and again very little alicyclic formation. However, the change in aromatic distribution is largely attributed to the breakdown and reforming of the Peneteck at this temperature.

The small peaks on the various chromatograms which are not numbered represent reaction intermediates and products not identified. These compounds may represent some one- to two percent of the total formed.

VI SUMMARY AND CONCLUSIONS

Analysis using vapor-phase chromatography shows that the destructive catalytic hydrogenation of quinoline probably takes place according to the following four reactions:

(1) 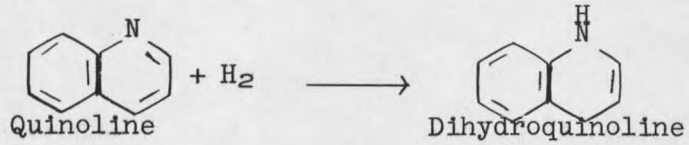

Quinoline — Dihydroquinoline

(2) 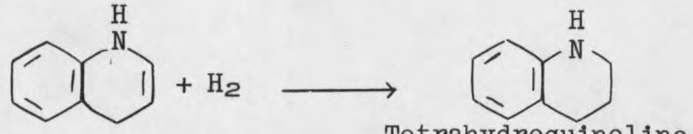

Tetrahydroquinoline

(3) 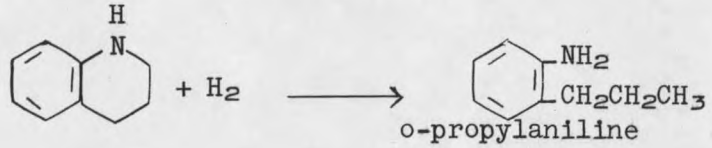

o-propylaniline

(4) 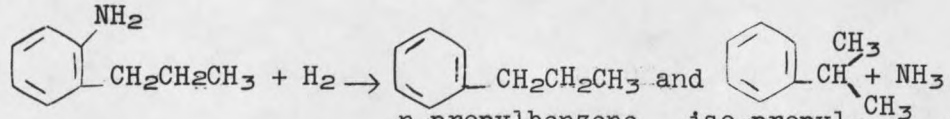

n-propylbenzene — iso-propylbenzene + ammonia

In addition, smaller amounts of other aniline homologs were formed which subsequently hydrogenated to their corresponding aromatic and alicyclic compounds.

The first three reactions appear to go much faster than the last one; at 50 percent conversion essentially all the nitrogen present is in the form of aniline derivatives. Thus, reaction (4)

is the slowest or rate controlling reaction. Furthermore, the rate controlling step will be one of the steps of reaction (4): hydrogenation of an amine in the form of an aniline derivative to yield an aromatic and ammonia. A simulated plot of mole fraction of each nitrogen compound present vs. reaction time is shown in Figure 25.

A number of reaction mechanisms corresponding to reaction (4) were postulated and tested on the basis of initial rates of reaction. On the basis of the experimental data, only the postulated mechanism of a dual site reaction between adsorbed amine and adsorbed molecular hydrogen could not be rejected. Thus, the reaction is thought to take place according to the following series of steps:

(1) $A + v \rightleftarrows Av$ $\qquad K_1 = C_A/P_A C_v$

(2) $H_2 + v \rightleftarrows H_2v$ $\qquad K_2 = CH_2/PH_2 C_v$

(3) $Av + H_2v \rightleftarrows Rv + Sv$ $\qquad K_3 = C_R C_S/C_A C_{H_2}$

(4) $Rv \rightleftarrows R + v$ $\qquad K_4 = P_R C_v/C_R$

(5) $Sv \rightleftarrows S + v$ $\qquad K_5 = P_S C_v/C_S$

with step (3), the surface reaction between the adsorbed molecules, controlling the overall rate of reaction.

The rate equation corresponding to this step controlling is:

$$r = \frac{kK_1K_2(P_A PH_2 - P_R P_S/K)}{(1 + K_1P_A + K_2PH_2 + P_R/K_4 + P_S/K_5 + K_6P_I)^2}$$

where the K_6P_I term is added to account for adsorption of the inert carrier oil on an active site.

It was found that empirically the reaction follows pseudo first order reaction kinetics when a large excess of hydrogen is used. The initial rates of reaction were calculated on the basis of this empirical correlation.

From the Arrhenius equation, the activation energy of the reaction was calculated. It was found to vary from 23.6 to 33.7 Kcal/mole as a linear function of pressure over the pressure range studied.

VII ACKNOWLEDGMENT

The author acknowledges with thanks the courtesy of the National Science Foundation, who for two year sponsored the fellowship under which this work was carried out.

He also wishes to thank the staff of the Chemical Engineering Department of Montana State College for their helpful suggestions and criticisms; in particular, Professor Lewis G. Mayfield, who directed this research.

VIII LITERATURE CITED

(1) Ball, J. S., et al., "Composition of Colorado Shale-Oil Naphtha", Ind. and Engr. Chem., 41:481 (1949).

(2) Ball, J. S., et al., "Nitrogen Content of Crude Petroleum", Ind. and Engr. Chem., 43:25 (1951).

(3) Barkely, L. W., et al., "Catalytic Reverse Shift Reaction", Ind. and Engr. Chem., 44:1066 (1952).

(4) Benson, D. B., Ph.D. Thesis, Montana State College, (1958).

(5) Berg, Clyde, "Advancements in Fuel Production from Shale Oil", Union Oil Co. (1954).

(6) Cady, W. E., and H. S. Seelig, "Composition of Shale Oil", Ind. and Engr. Chem., 44:2636 (1952).

(7) Casagrande, et al., "Selective Hydrotreating over Tungsten-Nickel Sulfide Catalyst", Ind. and Engr. Chem., 47:744 (1955).

(8) Clark, E. L., et al., "Hydrogenation of Shale-Oil Coker Distillate", Ind. and Engr. Chem., 43:2173 (1951).

(9) Corrigan, T. E., "Chemical Engineering Fundamentals", Chem. Engr., 61 (1954), 62 (1955).

(10) Cottingham, P. L., et al., "Hydrogenating Shale-Oil to Catalytic Reforming Stock", Ind. and Engr. Chem., 49:679 (1957).

(11) Cottingham, P. L., et al., "Hydrofining Thermally Cracked Shale-Oil Naphthas", Ind. and Engr. Chem., 48:1146 (1956).

(12) Daniels, F., Chemical Kinetics, Cornell Univ. Press, Ithaca, N. Y., (1938).

(13) Deal, Virginia, et al., "Determination of Basic Nitrogen in Oils", Anal. Chem., 25:426 (1953).

(14) Ellis, C. F., and J. D. Lankford, "Shale Oil Refining", Ind. and Engr. Chem., 43:27 (1951).

(15) Ellis, C. F., "The Chemistry of Petroleum Derivatives", Reinhold Publishing Company, New York (1937).

(16) Eyring, H., et al., "The Theory of Rate Processes", McGraw-Hill Book Co., Inc., New York (1941).

LITERATURE CITED (cont'd)

(17) Glasstone, Samuel, "Thermodynamics for Chemists", D. Van-Nostrand Co., Inc., New York (1954).

(18) Hodgeman, C. D., and H. N. Holmes, "Handbook of Chemistry and Physics", Chemical Rubber Publishing Co., Cleveland, Ohio, (1953).

(19) Holecek, R. J., M.S. Thesis, Montana State College, (1955).

(20) Hougen, O. A., and K. M. Watson, "Chemical Process Principles", John Wiley & Sons, Inc., New York (1947).

(21) Hougen, O. A., and K. H. Yang, "Determination of Mechanism of Catalyzed Gaseous Reactions", Chem. Engr. Prog., 46:146 (1950).

(22) Hull, W. Q., et al., "Liquid Fuels From Oil Shale", Ind. and Engr. Chem., 43:2 (1951).

(23) King, G. A., M.S. Thesis, Montana State College, (1955).

(24) Kirk, P. L., "Kjeldahl Method for Total Nitrogen", Analytical Chem., 22:354 (1950).

(25) Laidler, K. J., "Chemical Kinetics", McGraw-Hill Book Co., Inc., New York (1950).

(26) Lake, G. R., et al., "Effects of Digestion Temperature on Kjeldahl Analysis", Anal. Chem., 23:1632 (1951).

(27) Lange, Norbert A., "Handbook of Chemistry", Handbook Publishers, Inc., Sandusky, Ohio (1939).

(28) McKee, A. F., M.S. Thesis, Montana State College, (1956).

(29) McKee, R. H., "Shale Oil", The Chemical Catalogue Company, Inc., New York (1925).

(30) Mills, G. A., et al., "Chemical Characteristics of Catalysts. I. Poisoning of Cracking Catalysts by Nitrogen Compounds and Potassium Ion", J. Am. Chem. Soc., 72:1544, (1950).

(31) Nelson, W. L., "Petroleum Refinery Engineering", McGraw-Hill Book Company, Inc., New York (1949).

LITERATURE CITED (cont'd)

(32) Parks, G. S., et al., "Thermal Data on Organic Compounds", J. Am. Chem. Soc., 58:398 (1936).

(33) Perry, John H., "Chemical Engineers' Handbook", McGraw-Hill Book Co., Inc., New York (1950).

(34) Reid, R. C., and T. K. Sherwood, "The Properties of Gases and Liquids", McGraw-Hill Book Co., New York (1958).

(35) Scarborough, James B., "Numerical Mathematics Analysis", The Johns Hopkins Press, Baltimore (1955).

(36) Smith, J. M., "Chemical Engineering Kinetics", McGraw-Hill Book Co., New York (1956).

(37) Smith, J. M., "Introduction to Chemical Engineering Thermodynamics", McGraw-Hill Book Co., New York (1949).

(38) Stanfield, K. E., and H. M. Thorne, "Oil-Shale Research and Process Development", Ind. and Engr. Chem., 43:16 (1951).

(39) Thorne, H. M., et al., "Characteristics and Utilization of Oil Shale and Shale Oil", Ind. and Engr. Chem., 43:20 (1951).

(40) Twelfth Catalysis Report, John Wiley and Sons, New York (1940).

(41) United States Bureau of Mines, Report of Investigation, 4457 (1948).

(42) United States Bureau of Mines, Report of Investigation, 5044 (1951).

(43) Walas, Stanley M., "Reaction Kinetics for Chemical Engineers", McGraw-Hill Book Co., Inc., New York (1959).

(44) Wertheim, E., "Organic Chemistry", The Blakiston Co., New York (1951).

(45) Whitmore, F. C., "Organic Chemistry", D. Van Nostrand Co., Inc., New York (1951).

(46) "World Wide Oil Report", The Oil and Gas Journal, 57:53 (1959).

IX APPENDIX

APPENDIX (cont'd) page

APPENDIX (cont'd) page

Nomenclature (in consistent units)

a, b, c, d, e	constants
atm	atmospheres
bbl	barrels
eq	equilibrium
eu	entropy units
g	gaseous state (subscript)
k	forward reaction rate constant
k'	reverse reaction rate constant
k_e	empirical reaction rate constant
l	liquid state (subscript)
n	order of reaction
o	initial conditions (subscript)
p	partial pressure
psig	pounds per square inch, gauge
r	rate of reaction
s	frequency factor
t	time
v	a vacant site
x	amount converted
y	mole fraction
z	catalyst factor
A	Amine

Nomenclature (in consistent units)

A_i	Initial amount of Nitrogen
A, B	Reactants
C	Concentration
C_p	Heat Capacity, constant pressure
E_a	Energy of Activation
F	Free Energy
F	Feed Rate
H	Enthalpy
H_2	Hydrogen
H_v	Heat of Vaporization
I	Inert Component
K	Equilibrium Constant
M	Molecular Weight
N	Nitrogen
NE	Neutral Equilibrium
OD	Outside Diameter
P	Pressure
P_c	Critical Pressure
P_r	Reduced Pressure
Q	Quinoline
R	Universal Gas Constant
R, S	Products
S	Entropy

Nomenclature (in constant units)

S_v	Space Velocity, g/g hr
SCF	Standard Cubic Feet
T	Temperature
T_b	Temperature at Boiling Point
T_c	Critical Temperature
T_r	Reduced Temperature
V	Total Number of Active Sites
V	Volume
V_c	Critical Volume
W	Weight of Catalyst
γ	Activity Coefficient
Δ	Change
λ	Microliter
Θ	Parachor
Π	Total Pressure

Thermodynamic Study

The thermodynamic feasibility of the following overall reaction was studied at four pressures and four temperatures:

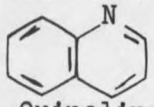

Quinoline + $4H_2$ (Hydrogen) $\longrightarrow$ ϕ-$CH_2CH_2CH_3$ (Propyl Benzene) + NH_3 (Ammonia)

Data which was needed for the calculations and was available in the literature are shown in Table I. Unless otherwise noted, the values are taken from the standard handbooks (18, 27, 33). Some data not available for quinoline also had to be estimated. This was: (1) the critical pressure, (2) the heat of vaporization, (3) the heat of formation in the gaseous state, and (4) the entropy in the gaseous state.

Most of the equations and methods of analysis used in this study can be found in such standard thermodynamics books as those by Smith, Glasstone, or Hougen and Watson (17, 20, 37). Other references are noted accordingly.

Critical Pressure: The critical pressure of quinoline was estimated by three different methods: Meissner-Redding, Riedel, and Lyderson (34). The Meissner-Redding method uses the equations:

$$V_2 = (0.377\,\Theta + 11.0)$$

and

$$P_c = \frac{20.8\ T_c}{V_c - 8}$$

The Riedel and Lyderson methods both use the equation:

$$P_c = \frac{M}{(\Theta + 0.33)^2}$$

In all cases, P_c is the critical pressure, V_c is the critical volume, T_c is the critical temperature, M is the molecular weight, and Θ is an atomic and structural parachor. The three methods give 39.3, 44.2, and 37.6 atmospheres, respectively. The average value of 40.4 was used in subsequent calculations.

Heat of Vaporization: The heat of vaporization of quinoline can be estimated from the equation (20):

$$\Delta H_{v298} = RT_b \ln P_c \frac{(1 - Tr_{298})^{0.38}}{(1 - Tr_b)^{1.38}}$$

where ΔH_{v298} is the heat of vaporization at 298°K, R is the universal gas constant, T_b is the temperature at the boiling point, and T_r is the reduced temperature defined as T/T_c. Evaluating this expression gives 13,120 cal/mole for the heat of vaporization at 298°K. Similarly, a value of 9,620 cal/mole was found for pyridine since it is needed in later calculations.

Heat of Formation: The heat of formation of quinoline in the gaseous state can be calculated from the equation:

$$\Delta H^\circ_{298(g)} = \Delta H^\circ_{298(l)} + \Delta H_{v298}$$

Evaluating this gives 48,770 cal/mole for the heat of formation.

Entropy: The entropy of quinoline in the gaseous state could be calculated from the equation:

$$S^\circ_{298(g)} = S^\circ_{298(l)} + \Delta H_{v298}/298 + R \ln P_{298}$$

if all the terms are known.

The entropy in the liquid state is known and the heat of vaporization has been calculated. However, the vapor pressure at 298°K is not available so this equation cannot be used.

The vapor pressure of pyridine is reported in Perry (33) as 20.2 mm of Hg at 298°K. Using the above equation, the entropy of pyridine in the gaseous state is calculated to be 68.9 eu/mole. This value can then be used to estimate the entropy of quinoline in the following manner. It is noted that the substitution of a nitrogen for a carbon in the benzene ring, forming pyridine from benzene, results in an entropy change of 4.56 eu/mole. Assume that this same difference results in the substitution of a nitrogen into the naphthalene ring to form quinoline. This can be represented as follows:

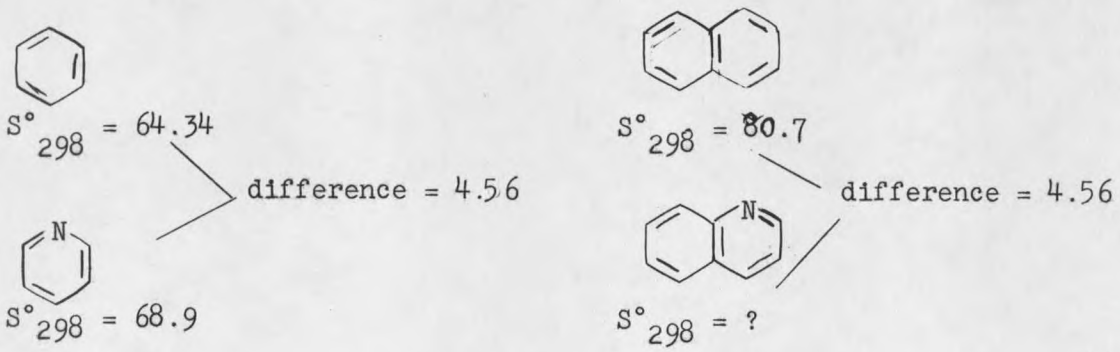

Thus, adding 4.56 to 80.7, the entropy of quinoline in the gaseous state is estimated to be 85.26 eu/mole.

Calculations: The heat of reaction is calculated from the equation:

$$\Delta H^\circ_{298} = \Delta H^\circ_{f298(\text{products})} - \Delta H^\circ_{f298(\text{reactants})}$$

to give $\Delta H^\circ_{298} = \left[1{,}870 + (-11{,}030)\right] - \left[48{,}770 + 4(0)\right] = -57{,}930$ cal/mole

The change in entropy is calculated from the equation:

$$\Delta S^\circ_{298} = S^\circ_{298(\text{products})} - S^\circ_{298(\text{reactants})}$$

to give $\Delta S^\circ_{298} = \left[(95.76 + 46.03)\right] - \left[(85.26 + 4(31.21)\right] = -68.31$ eu/mole.

These values are then used to calculate the standard free energy change from the equation:

$$\Delta F^\circ_t = \Delta H^\circ_t - T \Delta S^\circ_t$$

to give $\Delta F^\circ_{298} = -57{,}930-(298)(-68.31) = -37{,}580$ cal/mole

At neutral equilibrium the free energy change is zero and the above equation can be written:

$$\Delta H^\circ - T \Delta S^\circ = 0$$

or

$$T_{NE} = \Delta H^\circ_{NE} / \Delta S^\circ_{NE}$$

Using ΔH°_{298} and ΔS°_{298}, the temperature of neutral equilibrium is approximated to be:

$$T_{NE} = -57,930/-68.31 = 850°K$$

The free energy change at other temperatures is calculated by re-writing the free energy equation as:

$$\Delta F^\circ_t = \Delta H^\circ_{298} + \int \Delta C_p dT - T\left(\Delta S^\circ_{298} + \int C_p dT/T\right)$$

However, heat capacity data on quinoline are unavailable, so the above equation is written in the approximate form:

$$\Delta F^\circ_t = \Delta H^\circ_{298} - T \Delta S^\circ_{298}$$

The free energy change was calculated at four temperatures and the corresponding equilibrium constants calculated from the equation:

$$\ln K_{eq} = -\Delta F^\circ/RT$$

These values are tabulated in Table II.

The equilibrium conversion can be calculated as follows:

Let x be the moles of quinoline reacted at equilibrium. Then the moles of each component present are:

moles of quinoline =	$1 - x$
moles of hydrogen =	$4(1 - x)$
moles of ammonia =	x
moles of propyl benzene =	x
total moles =	$5 - 3x$

and the mole fractions of each component are:

$$y_Q = 1 - x/5 - 3x$$

$$y_H = 4(1 - x)/5 - 3x$$

$$y_A = y_P = x/5 - 3x$$

where the subscripts Q, H, A, and P are quinoline, hydrogen, ammonia, and propyl benzene, respectively. These values are then substituted into the equation:

$$K_y K_\gamma = K_{eq} P^{\Delta n}$$

where $K_y = y_A y_P / y_Q y_H^4$, $K_\gamma = \gamma_A \gamma_P / \gamma_Q \gamma_H^4$, Δn = moles of reactants minus moles of products, and γ is the activity coefficient calculated from the relationship:

$$\ln \gamma = 9/128 \; PT_c/TP_c \left[1 - 6(T_c/T)^2\right]$$

This equation then reduces to:

$$K_N = x^2(5 - 3x)^3/256(1 - x)^5 = K_{eq} P^3/K_\gamma$$

Solving for x and then forming the ratio $x/5 - 3x$, the maximum conversion that can be expected at a given set of conditions is obtained. The calculated activity coefficients are tabulated in Table III and the conversions with related quantities in Table IV.

TABLE I

THERMODYNAMIC DATA

Compound	T_c (°K)	P_c (atm)	H°_{f298} (cal/mole)	S°_{298} (eu/mole)
Propyl Benzene	639	32.3	1,870(g)	95.76(g)
Ammonia	405	111.5	-11,030(g)	46.03(g)
Hydrogen	33	12.8	0	31.21(g)
Quinoline (32)	793		35,650(l)	92.5 (l)
Pyridine (32)	617	60.0	17,920(l)	65.0 (l)
Benzene	-	-	-	64.34(g)
Naphthalene	-	-	-	80.7 (g)

TABLE II

FREE ENERGY CHANGE AND EQUILIBRIUM CONSTANTS

Temp. (°K)	F° (cal/mole)	K_{eq}
300	-37,580	1.5×10^{27}
500	-23,830	2.4×10^{10}
700	-10,150	1.4×10^{3}
1000	10,380	5.6×10^{-3}

TABLE III

ACTIVITY COEFFICIENTS

Press. (atm)	Temp. (°K)	γ H	γ Q	γ N	γ P
1	300	1.000	0.830	0.994	0.886
	500	1.000	0.964	1.000	0.976
	700	1.000	0.989	1.000	0.994
	1000	1.000	0.998	1.000	1.000
10	300	1.000	0.153	0.920	0.296
	500	1.000	0.679	0.987	0.785
	700	1.000	0.878	0.999	0.920
	1000	1.000	0.965	1.000	0.982
50	300	1.003	8.33×10^{-5}	0.656	0.00226
	500	1.002	0.144	0.930	0.295
	700	1.001	0.519	0.984	0.672
	1000	1.000	0.828	1.000	0.905
200	300	1.011	4.8×10^{-17}	0.185	2.6×10^{-11}
	500	1.007	4.27×10^{-4}	0.742	0.0075
	700	1.005	0.0718	0.925	0.204
	1000	1.004	0.466	1.000	0.669

TABLE IV

THERMODYNAMIC STUDY RESULTS

Press. (atm)	Temp. (°K)	K_{eq}	K_{γ}	K_N	% Conversion
I	300	1.5×10^{27}	1.061	1.41×10^{27}	99.9
	500	2.4×10^{10}	1.012	2.37×10^{10}	99.5
	700	1.4×10^{3}	1.006	1.39×10^{3}	87.8
	1000	5.6×10^{-3}	1.002	5.6×10^{-3}	9.3
10	300	5.6×10^{-3}	1.781	8.4×10^{29}	99.9
	500	5.6×10^{-3}	1.141	2.10×10^{13}	99.8
	700	5.6×10^{-3}	1.048	1.34×10^{6}	97.0
	1000	5.6×10^{-3}	1.018	5.50	61.6
50	300	5.6×10^{-3}	17.55	1.07×10^{31}	99.9
	500	5.6×10^{-3}	1.890	1.59×10^{15}	99.9
	700	5.6×10^{-3}	1.270	1.37×10^{8}	98.9
	1000	5.6×10^{-3}	1.092	6.41×10^{2}	86.0
200	300	5.6×10^{-3}	9580.	1.25×10^{32}	99.9
	500	5.6×10^{-3}	12.68	1.52×10^{18}	99.9
	700	5.6×10^{-3}	2.575	4.35×10^{9}	99.2
	1000	5.6×10^{-3}	1.413	3.17×10^{4}	93.5

TABLE V

CONVERSION-TIME DATA

Sample No.	Hrs. on Stream	A-x	A-x/A	x/A
1	2	0.670	0.613	0.387
2	3	0.788	0.720	0.280
3	4	0.842	0.769	0.231
4	5	0.854	0.779	0.221
5	6	0.873	0.796	0.204
6	7	0.873	0.796	0.204
7	8	0.894	0.816	0.184
8	10	0.891	0.814	0.186
9	12	0.895	0.816	0.184
10	14	0.896	0.817	0.183
11	16	0.894	0.816	0.184
12	18	0.904	0.824	0.176
13	20	0.900	0.823	0.177
14	22	0.905	0.825	0.175
15	25	0.907	0.828	0.172
16	28	0.905	0.825	0.175

Uniform Operating Conditions for Run 7:

Pressure: 250 psig
Temperature: 725°F (385°C)
Space Velocity: 0.5 g/g hr
Hydrogen Rate: 7500 SCF/bbl
Initial Nitrogen: 1.095 wt. % N
Weight of Catalyst: 100 g.

TABLE VI

FILM DIFFUSION DATA

Run No.	g. of Catalyst	A-x	A-x/A	x/A
8	15	0.736	0.672	0.328
9	25	0.730	0.668	0.332
10	50	0.750	0.685	0.315
11	75	0.738	0.674	0.326

Uniform Operating Conditions:

Pressure: 1000 psig
Temperature: 725°F (385°C)
Space Velocity: 2.0 g/g hr
Hydrogen Rate: 7500 SCF/bbl
Initial Nitrogen: 1.095 wt. % N

TABLE VII

INTERNAL DIFFUSION DATA

Run No.	Catalyst Size	A-x	A-x/A	x/A
12	16-35 mesh	0.648	0.592	0.408
13	10-16 mesh	0.654	0.596	0.404
14	1/8-in. pellets	0.640	0.585	0.415

Uniform Operating Conditions:

Pressure: 500 psig
Temperature: 725°F (385°C)
Space Velocity: 0.5 g/g hr
Hydrogen Rate: 7500 SCF/bbl
Initial Nitrogen: 1.095 % N
Weight of Catalyst: 100 g

TABLE VIII. EMPIRICAL RATE EQUATION DATA

Run No.	Press. (psig)	Grams Catalyst	Space Vel.	A-x	1/A-x	A/A-x	ln A/A-x	A-x/A	x/A
15	250	100	1/3	0.832	1.202	1.317	0.275	0.760	0.240
7	250	100	1/2	0.890	1.123	1.230	0.207	0.813	0.187
16	250	50	1.0	1.013	0.986	1.018	0.080	0.925	0.075
17	250	25	2.0	1.038	0.964	1.055	0.052	0.948	0.052
18	250	25	4.0	1.063	0.939	1.028	0.028	0.971	0.029
19	500	100	1/3	0.480	2.083	2.280	0.824	0.438	0.562
12	500	100	1/2	0.648	1.542	1.690	0.525	0.592	0.408
13	500	100	1/2	0.654	1.530	1.675	0.515	0.596	0.404
14	500	100	1/2	0.640	1.563	1.711	0.537	0.585	0.415
20	500	50	1.0	0.846	1.182	1.295	0.258	0.773	0.227
21	500	25	2.0	0.948	1.054	1.153	0.142	0.866	0.134
22	500	25	4.0	1.038	0.964	1.055	0.052	0.948	0.052
23	1000	100	1/2	0.250	4.000	4.380	1.477	0.228	0.772
24	1000	50	1.0	0.526	1.902	2.082	0.733	0.480	0.520
8	1000	15	2.0	0.736	1.358	1.485	0.395	0.672	0.328
9	1000	25	2.0	0.730	1.370	1.500	0.405	0.668	0.332
10	1000	50	2.0	0.750	1.333	1.460	0.378	0.685	0.315
11	1000	75	2.0	0.738	1.355	1.482	0.394	0.674	0.326
25	1000	25	4.0	0.832	1.202	1.317	0.275	0.760	0.240
26	1000	15	10.0	1.010	0.990	1.083	0.080	0.922	0.078

Uniform Operating Conditions:

Temperature: 725°F (385°C)
Hydrogen Rate: 7500 SCF/bbl
Initial Nitrogen: 1.095 Wt. % N

TABLE IX

ACTIVATION ENERGY DATA

Run No.	Press. (psig)	Temp. °F	Temp. °C	°K	$\frac{1}{T} \times 10^3$	A-x	A/A-x	k_e ln A/A-x	ln k_e
7,15 -18	250	725	385	658	1.520	---	---	0.0944	-2.359
27	250	750	399	672	1.488	0.938	1.168	0.1560	-1.858
28	250	775	413	686	1.458	0.838	1.308	0.2685	-1.315
29	250	800	427	700	1.429	0.698	1.568	0.4498	-0.799
12-14 19-22	500	725	385	658	1.520	---	---	0.2675	-1.318
30	500	750	399	672	1.488	0.704	1.556	0.4421	-0.816
31	500	775	413	686	1.458	0.541	2.025	0.7055	-0.349
32	500	800	427	700	1.429	0.220	4.970	1.6030	0.472
8-11 23-26	1000	725	385	658	1.520	---	---	0.7502	-0.287
33	1000	750	399	672	1.488	0.361	3.040	1.1118	0.106
34	1000	775	413	686	1.458	0.222	4.930	1.595	0.467
35	1000	800	427	700	1.429	0.056	19.560	2.974	1.090

Uniform Operating Conditions:

Space Velocity: 1.0 g/g hr
Hydrogen Rate: 7500 SCF/bbl
Initial Nitrogen: 1.095 wt. % N

TABLE X

INITIAL RATES FOR CONSTANT FEED COMPOSITION

Run No.	Temp. °F	Press. (psig)	k_e	r_o	$\frac{\pi^2}{r_o}$	$\sqrt{\frac{\pi^2}{r_o}}$
7 15-18	725	250	0.0944	0.1033	6.76×10^5	8.21×10^2
12-14 19-22	725	500	0.2675	0.2925	9.05×10^5	9.52×10^2
8-11 23-26	725	1000	0.7502	0.821	12.55×10^5	11.17×10^2
27	750	250	0.1560	0.1708	4.10×10^5	6.40×10^2
30	750	500	0.4421	0.484	5.46×10^5	7.38×10^2
33	750	1000	1.1118	1.223	8.42×10^5	9.18×10^2
28	775	250	0.2685	0.294	2.38×10^5	4.88×10^2
31	775	500	0.7055	0.772	3.43×10^5	5.85×10^2
34	775	1000	1.595	1.747	5.89×10^5	7.67×10^2

Uniform Operating Conditions:

Space Velocity: 1.0 g/g hr
Hydrogen Rate: 7500 SCF/bbl
Initial Nitrogen: 1.095 Wt. % N

TABLE XI

INITIAL RATES FOR VARIABLE FEED COMPOSITION

Run No.	A Wt. % N	A-x	A/A-x	ln A/A-x	k_e	r_o
36	0.268	0.0305	8.770	2.171	1.085	0.291
37	0.538	0.168	3.205	1.166	0.583	0.313
12-14 19-22	1.095	---	---	---	0.2675	0.293
38	1.940	0.159	1.218	0.1970	0.0985	0.191

Uniform Operating Conditions:

Pressure: 500 psig
Temperature: 725°F (385°C)
Space Velocity: 1/2 g/g hr
Hydrogen Rate: 7500 SCF/bbl

TABLE XII

POSTULATED MECHANISMS

I. Reaction between molecularly adsorbed hydrogen and adsorbed amine.

(a) $A + v \rightleftarrows Av$

(b) $H_2 + v \rightleftarrows H_2v$

(c) $Av + H_2v \rightleftarrows Rv + Sv$

(d) $Rv \rightleftarrows R + v$

(e) $Sv \rightleftarrows S + v$

II. Reaction between atomically adsorbed hydrogen and adsorbed amine.

(f) $A + v \rightleftarrows Av$

(g) $H_2 + 2v \rightleftarrows 2Hv$

(h) $Av + 2Hv \rightleftarrows Rv + Sv + v$

(i) $Rv \rightleftarrows R + v$

(j) $Sv \rightleftarrows S + v$

III. Reaction between molecularly adsorbed hydrogen and amine in the gas phase.

(k) $H_2 + v \rightleftarrows H_2v$

(l) $A + H_2v \rightleftarrows Rv + S$

(m) $Rv \rightleftarrows R + v$

IV. Reaction between atomically adsorbed hydrogen and amine in the gas phase.

(n) $H_2 + 2v \rightleftarrows 2Hv$

(o) $A + 2Hv \rightleftarrows Rv + Sv$

(p) $Rv \rightleftarrows R + v$

(q) $Rv \rightleftarrows R + v$

TABLE XII (cont'd).

POSTULATED MECHANISMS

V. Reaction between hydrogen in gas phase and adsorbed amine.

(r) $A + v \rightleftarrows Av$

(s) $Av + H_2 \rightleftarrows Rv + S$

(t) $Rv \rightleftarrows R + v$

TABLE XIII

INITIAL RATE EQUATIONS

Mechanism		Equation
I.	(a)	$r_o = \frac{P_A}{a + bP_{H_2} + dP_I}$
	(b)	$r_o = \frac{P_{H_2}}{a + cP_A + dP_I}$
	(c)	$r_o = \frac{P_{H_2}}{(a + bP_{H_2} + cP_A + dP_I)^2}$
	(d), (e)	$r_o = a$
II.	(f)	$r_o = \frac{P_A}{a + b\sqrt{P_{H_2}} + dP_I}$
	(g)	$r_o = \frac{P_{H_2}}{(a + cP_A + dP_I)^2}$
	(h)	$r_o = \frac{P_A P_{H_2}}{(a + b\sqrt{P_{H_2}} + cP_A + dP_I)^3}$
	(i), (j)	$r_o = a$
III.	(k)	$r_o = bP_{H_2}$
	(l)	$r_o = \frac{P_A P_{H_2}}{a + bP_{H_2} + dP_I}$

TABLE XIII (cont'd).

INITIAL RATE EQUATIONS

	Mechanism	Equation
	(m)	$r_o = a$
IV.	(n)	$r_o = bP_{H_2}$
	(o)	$r_o = \frac{P_A P_{H_2}}{(a + b\sqrt{P_{H_2}} + dP_I)^2}$
	(p) & (q)	$r_o = a$
V.	(r)	$r_o = cP_A$
	(s)	$r_o = \frac{P_A P_{H_2}}{a + cP_A + dP_I}$
	(t)	$r_o = a$

TABLE XIV

INITIAL RATE EQUATIONS FOR CONSTANT FEED COMPOSITION

Mechanism		Equation
I.	(a), (b)	$r_o = \frac{\pi}{a' + b'}$
	(c)	$r_o = \frac{\pi^2}{(a' + b' \pi)^2}$
	(d), (e)	$r_o = a'$
II.	(f)	$r_o = \frac{\pi}{a' + b' \sqrt{\pi} + c' \pi}$
	(g)	$r_o = \frac{\pi}{(a' + b' \pi)^2}$
	(h)	$r_o = \frac{\pi^2}{(a' + b' \sqrt{\pi} + c \pi)^3}$
	(i), (j)	$r_o = a'$
III.	(k)	$r_o = a' \pi$
	(l)	$r_o = \frac{\pi^2}{a' + b' \pi}$

TABLE XIV (cont'd).

INITIAL RATE EQUATIONS FOR CONSTANT FEED COMPOSITION

	Mechanism	Equation
	(m)	$r_o = a'$
IV.	(n)	$r_o = a' \pi$
	(o)	$r_o = \frac{\pi^2}{(a' + b'\sqrt{\pi} + c'\pi)^2}$
	(p), (q)	$r_o = a'$
V.	(r)	$r_o = a'\pi$
	(s)	$r_o = \frac{\pi^2}{a' + b'\pi}$
	(t)	$r_o = a'$

TABLE XV

INITIAL RATE FUNCTIONS FOR VARIABLE FEED COMPOSITION

Run No.	r_o	y_A	y_H	$y_A y_H$	$\frac{y_A y_H}{r_o}$	$\left(\frac{y_A y_H}{r_o}\right)^{1/2}$	$\left(\frac{y_A y_H}{r_o}\right)^{1/3}$
36	0.291	0.00244	0.943	0.0023	0.00791	0.0890	0.199
37	0.313	0.00487	0.942	0.0046	0.0147	0.1210	0.244
12-14 19-22	0.293	0.00990	0.940	0.00996	.0340	0.1842	0.324
38	0.191	0.0174	0.937	0.0163	0.0853	0.292	0.440

Conversion Data are shown in Table XI.

Uniform Operating Conditions:

Pressure: 500 psig
Temperature: 725°F (385°C)
Space Velocity: 0.5 g/g hr
Hydrogen Rate: 7500 SCF/bbl

TABLE XVI

RUN DATA USING CETANE AS CARRIER OIL

Run No.	Space Velocity	Grams Catalyst	A-x	x/A
39-c	2.0	25	1.292	0.097
40-c	0.5	100	0.680	0.542
41-c	~0.2	100	0.056	0.962

Uniform Operating Conditions:

Pressure: 500 psig
Temperature: 725°F (385°C)
Hydrogen Rate: 7500 SCF/bbl for Runs 39, 40
~20,000 SCF/bbl for Run 41
Initial Nitrogen: 1.435 Wt. % N for Run 39
1.483 Wt. % N for Runs 40, 41

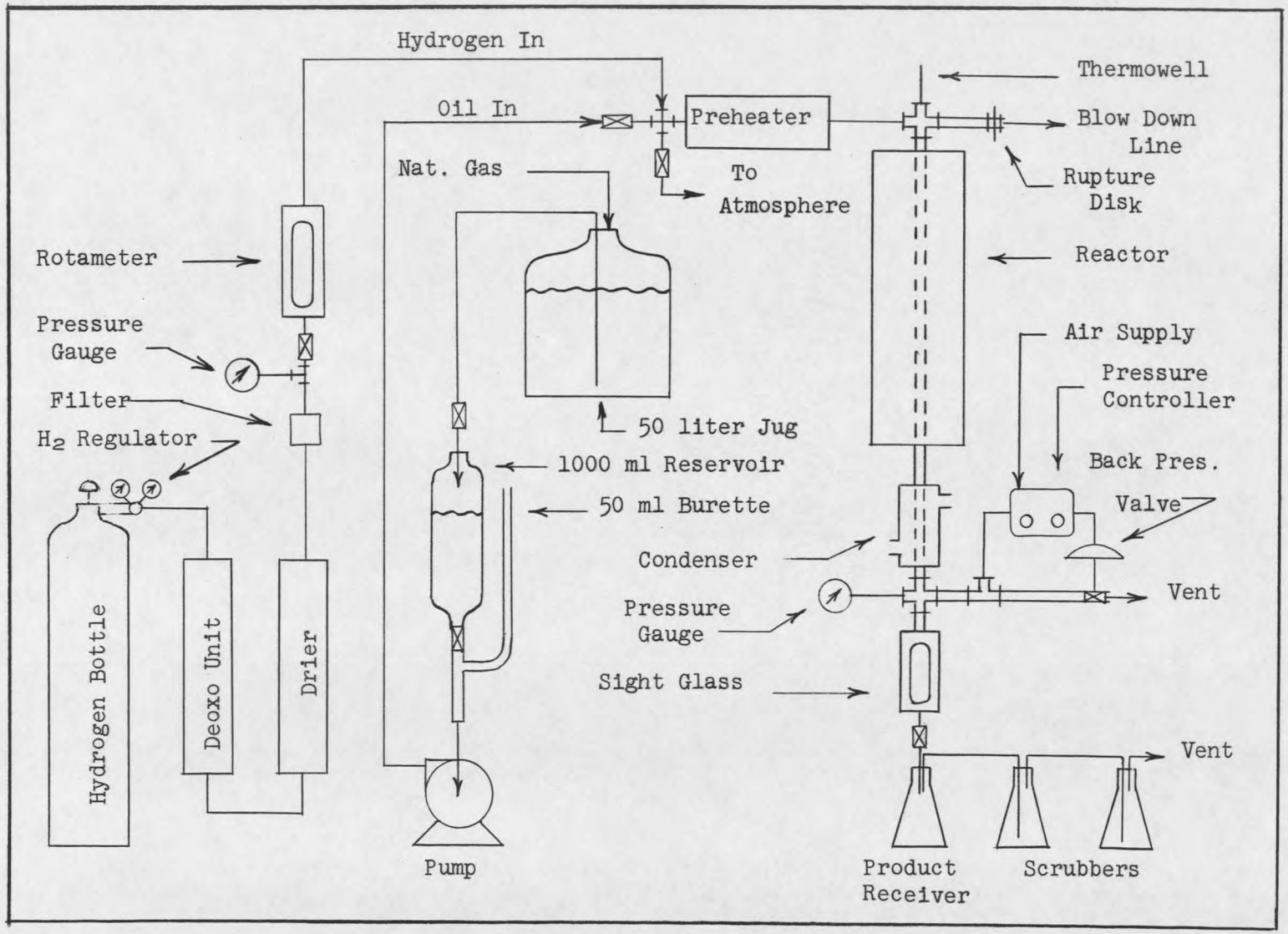

Figure 1. Schematic Flow Diagram of the Processing Unit

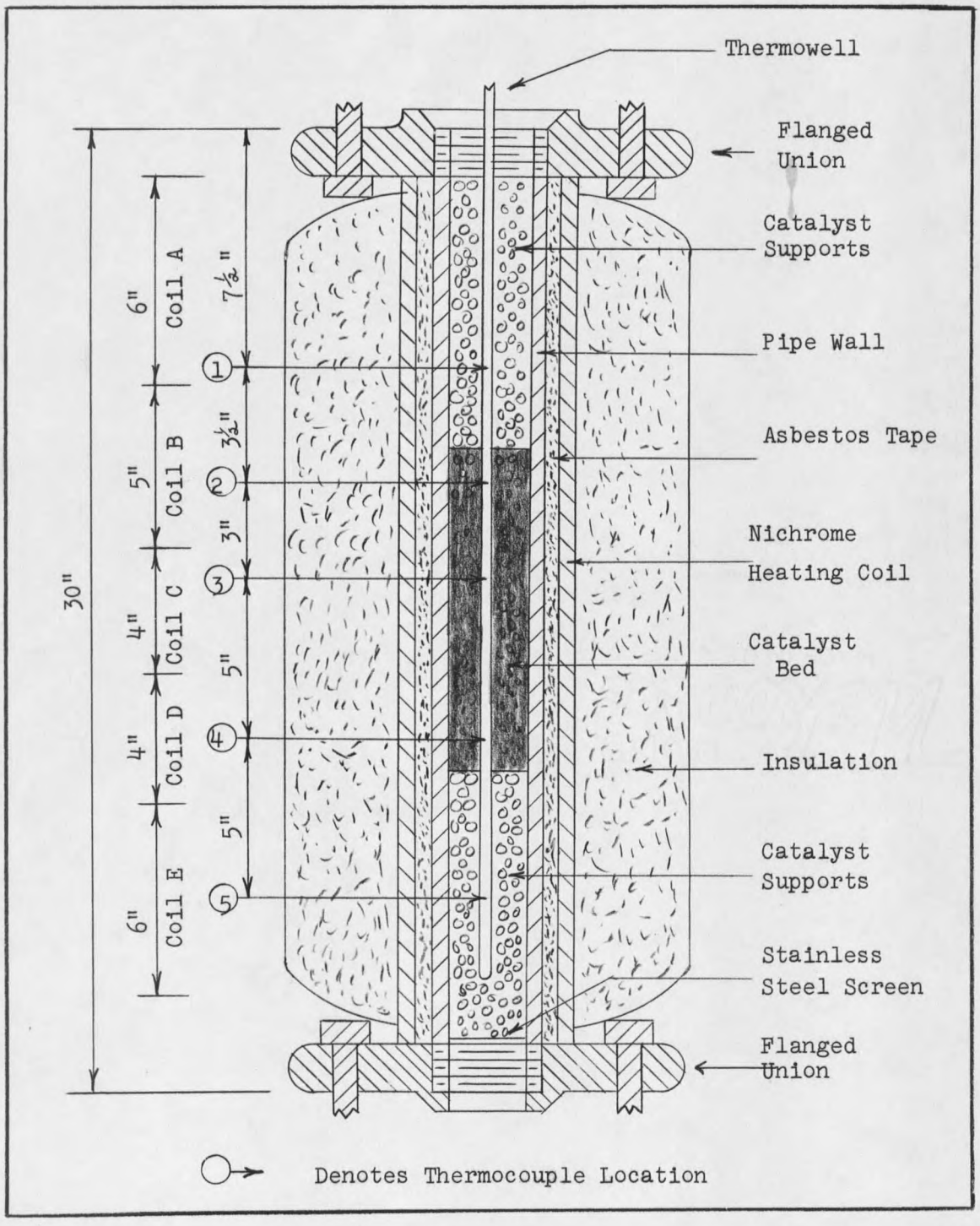

Figure 2. Detailed Diagram of Reactor

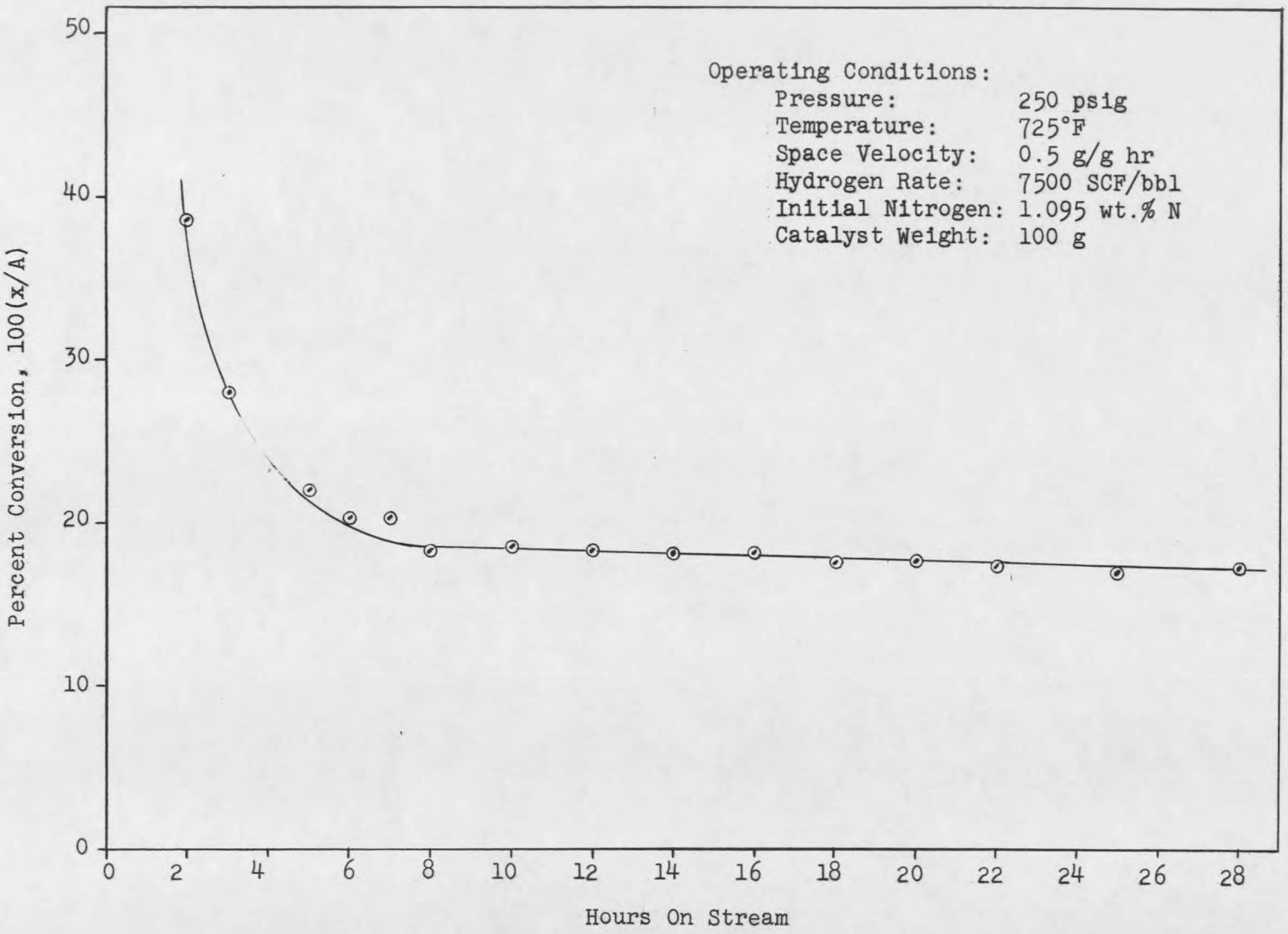

Figure 3. Conversion vs. Hours on Stream to Determine Length of Run Necessary for Line-out

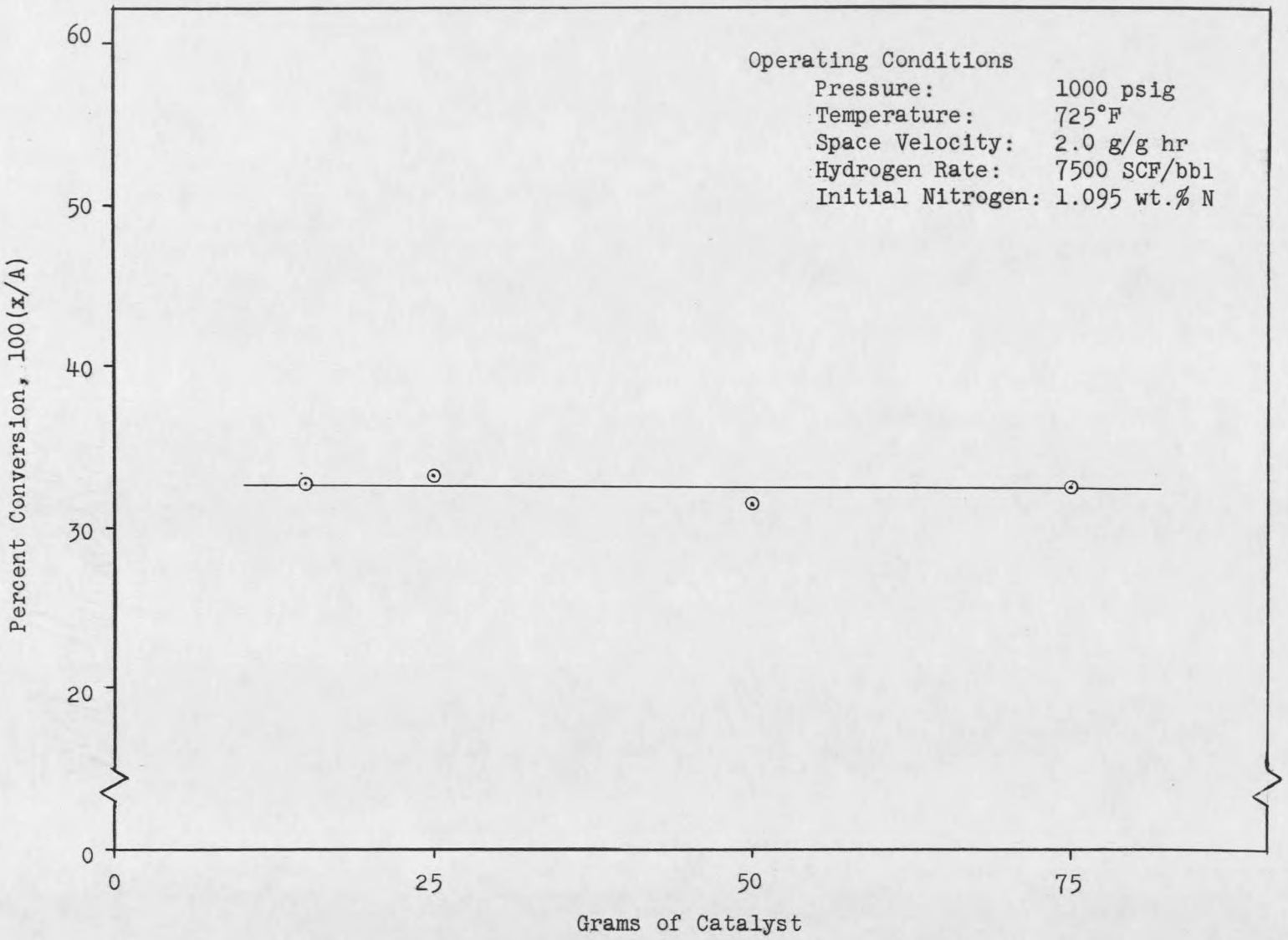

Figure 4. Conversion vs. Grams of Catalyst to Test for Film Diffusion Controlling

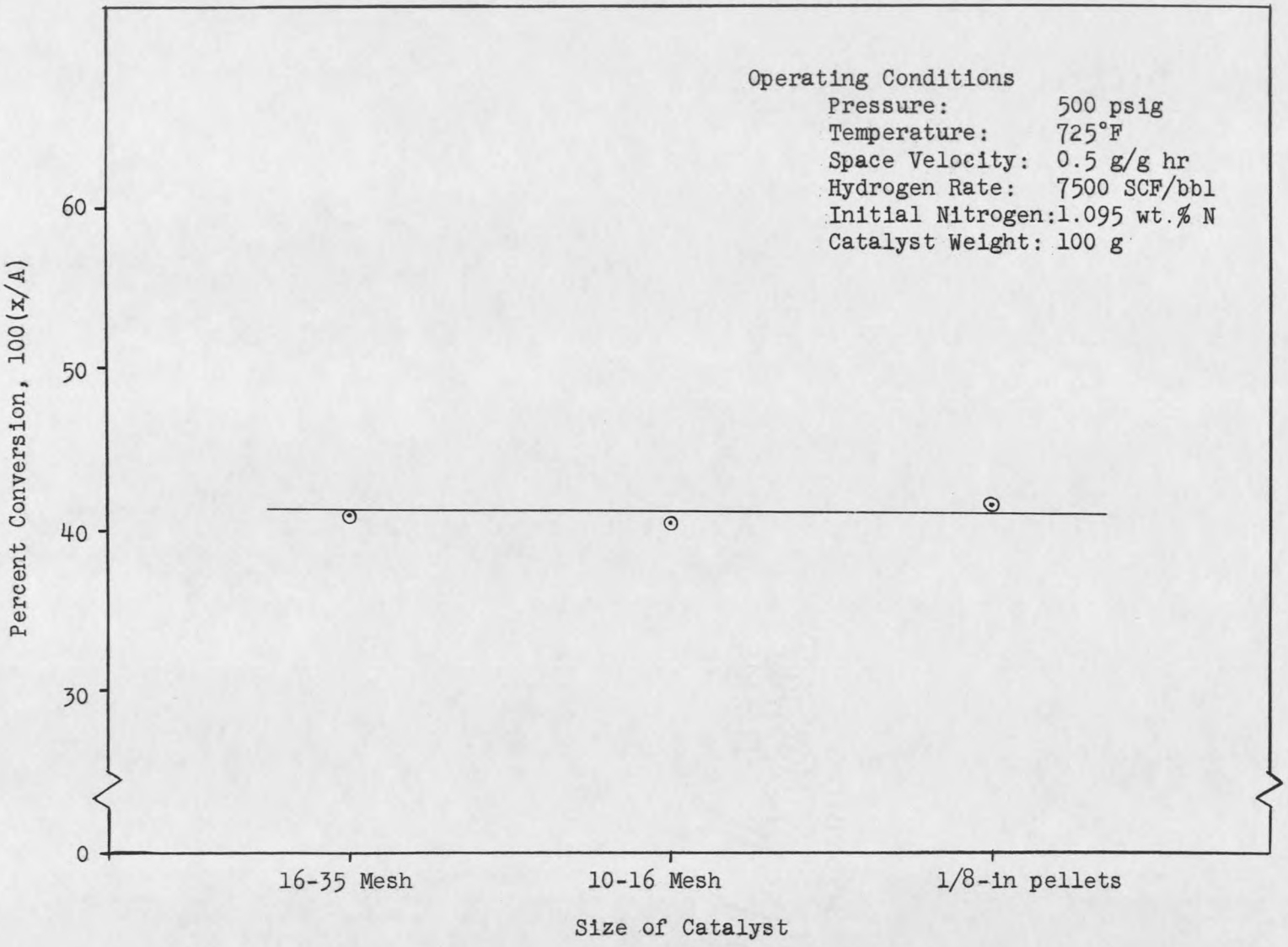

Figure 5. Conversion vs. Size of Catalyst to Test for Internal Diffusion Controlling

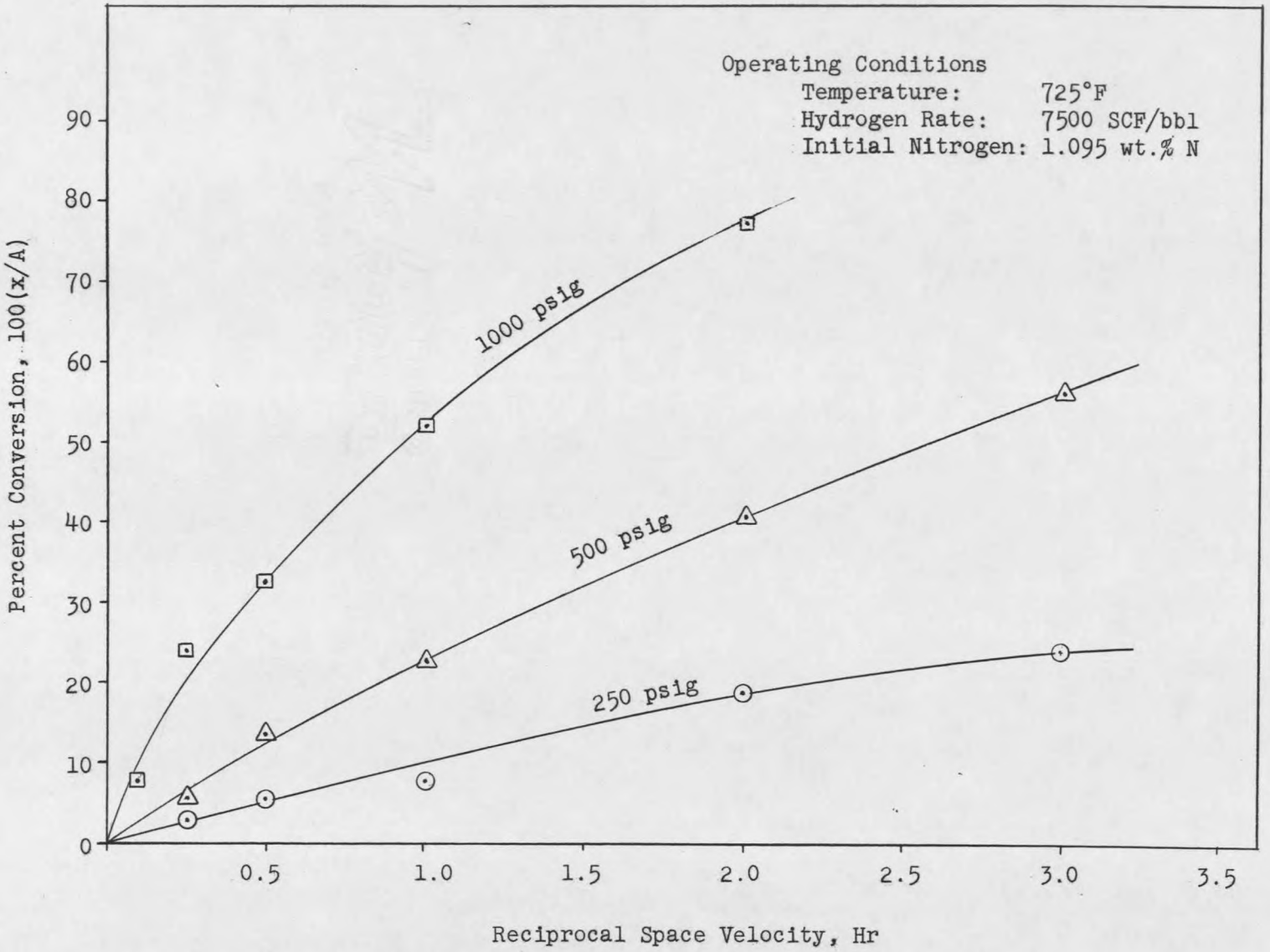

Figure 6. Conversion vs. Reciprocal Space Velocity Showing Effect of Pressure

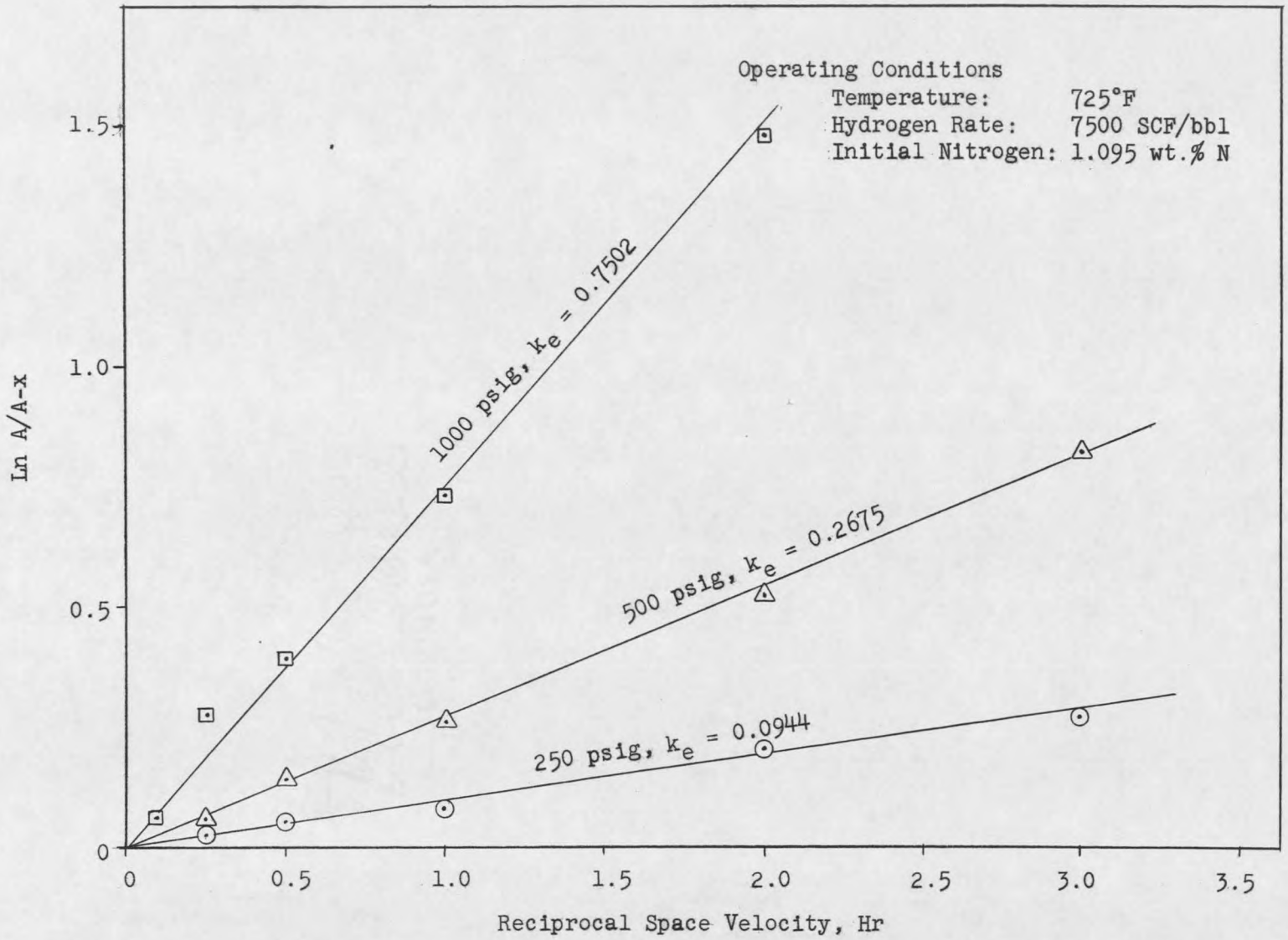

Figure 7. Plot of Ln A/A-x vs. Reciprocal Space Velocity to Test for Pseudo First Order Reaction

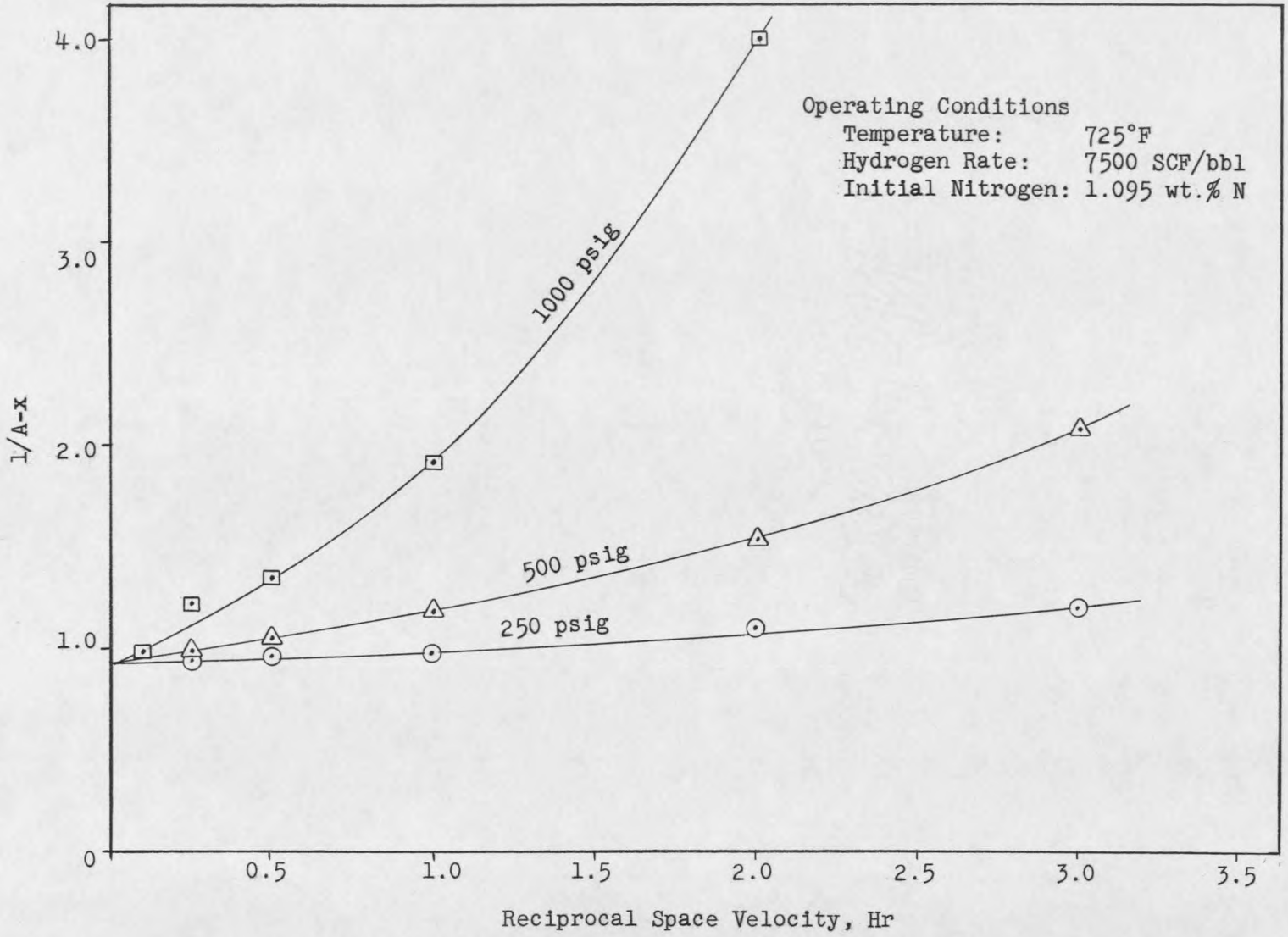

Figure 8. Plot of 1/A-x vs. Reciprocal Space Velocity to Test for Pseudo Second Order Reaction

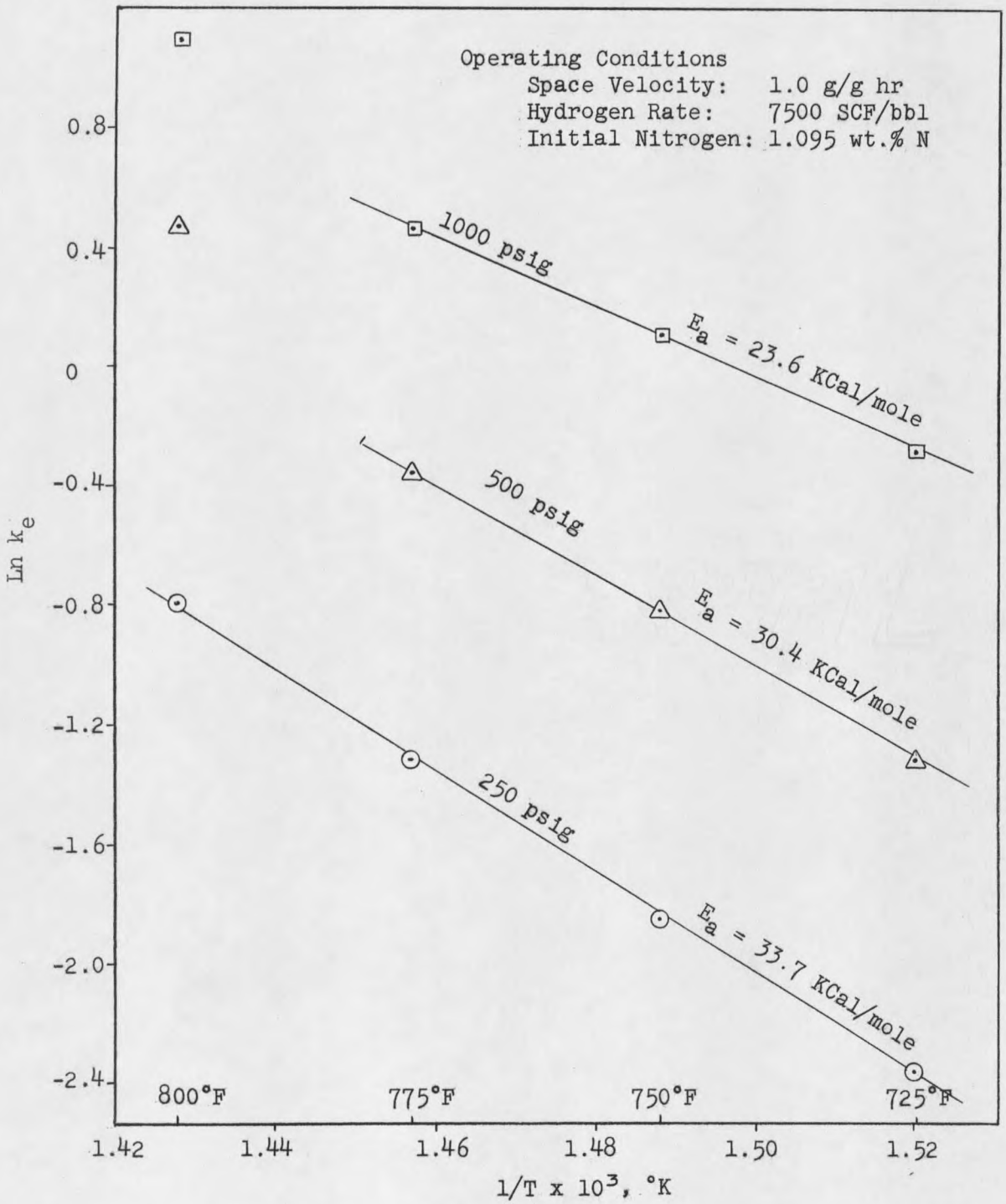

Figure 9. Plot of Ln k_e vs. 1/T to Determine Activation Energies.

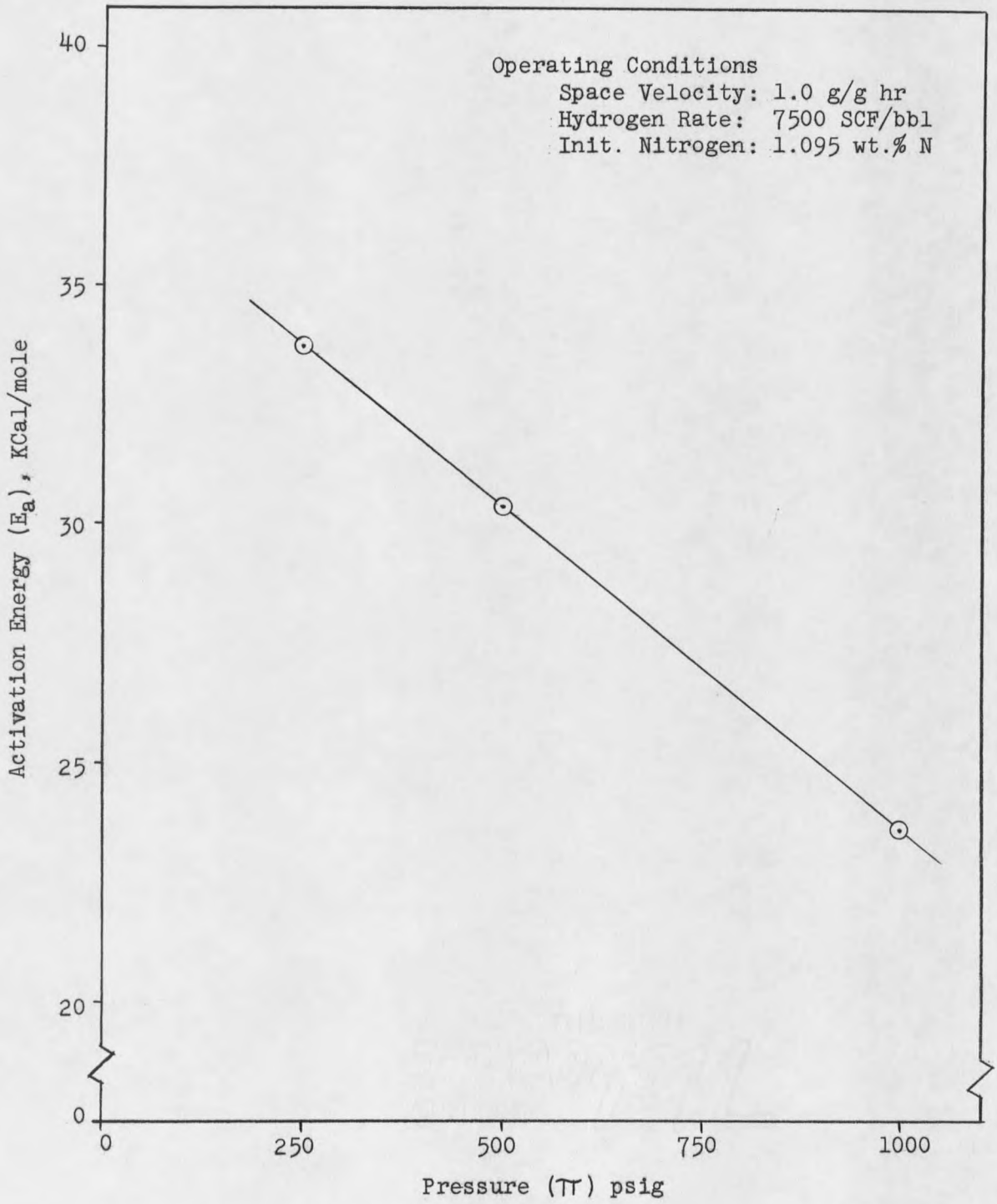

Figure 10. Plot of Activation Energy vs. Pressure

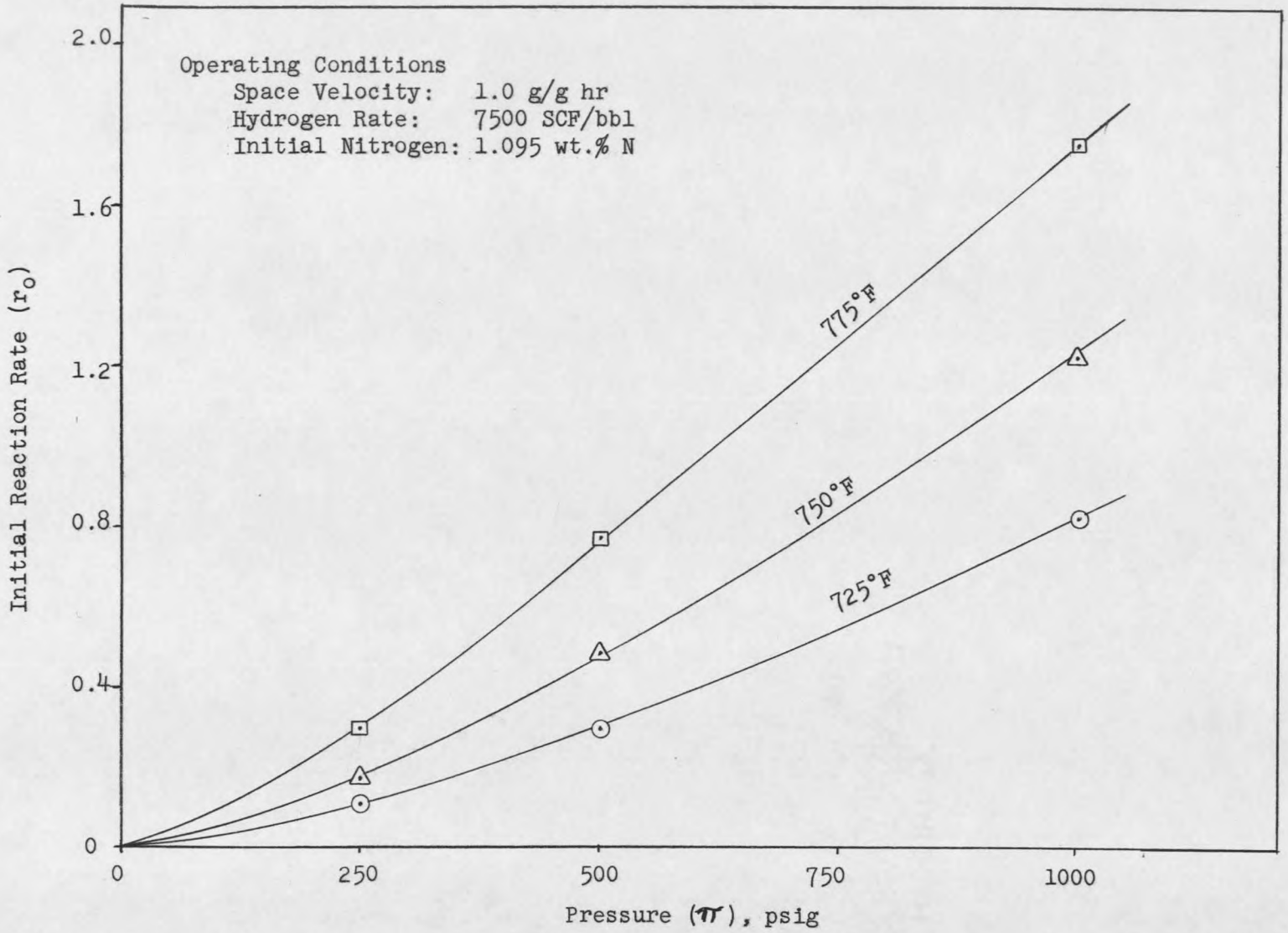

Figure 11. Plot of Initial Reaction Rate vs. Pressure for Various Temperatures

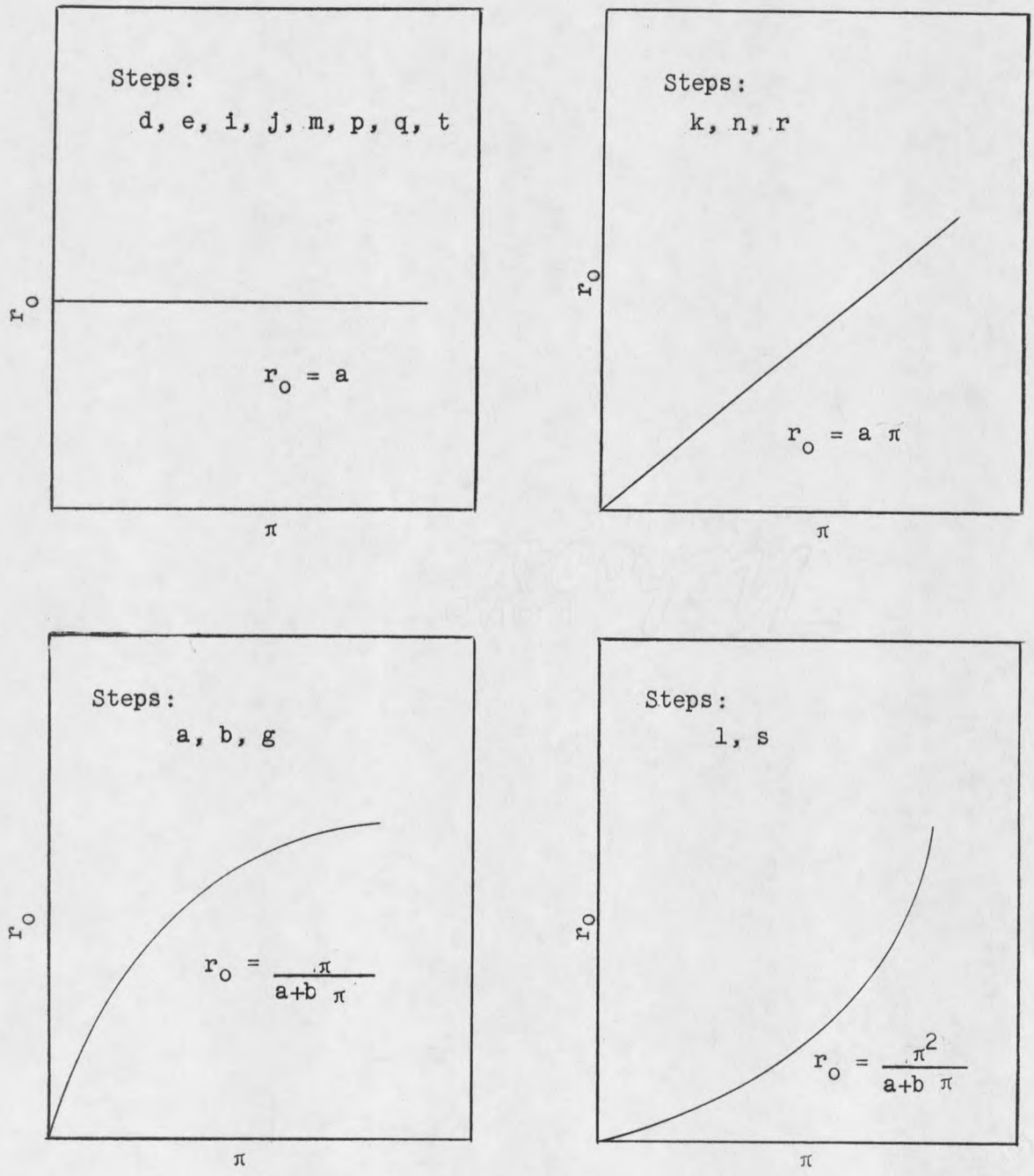

Figure 12. Graphs of Initial Reaction Rate Equations for Each Step Rate Controlling

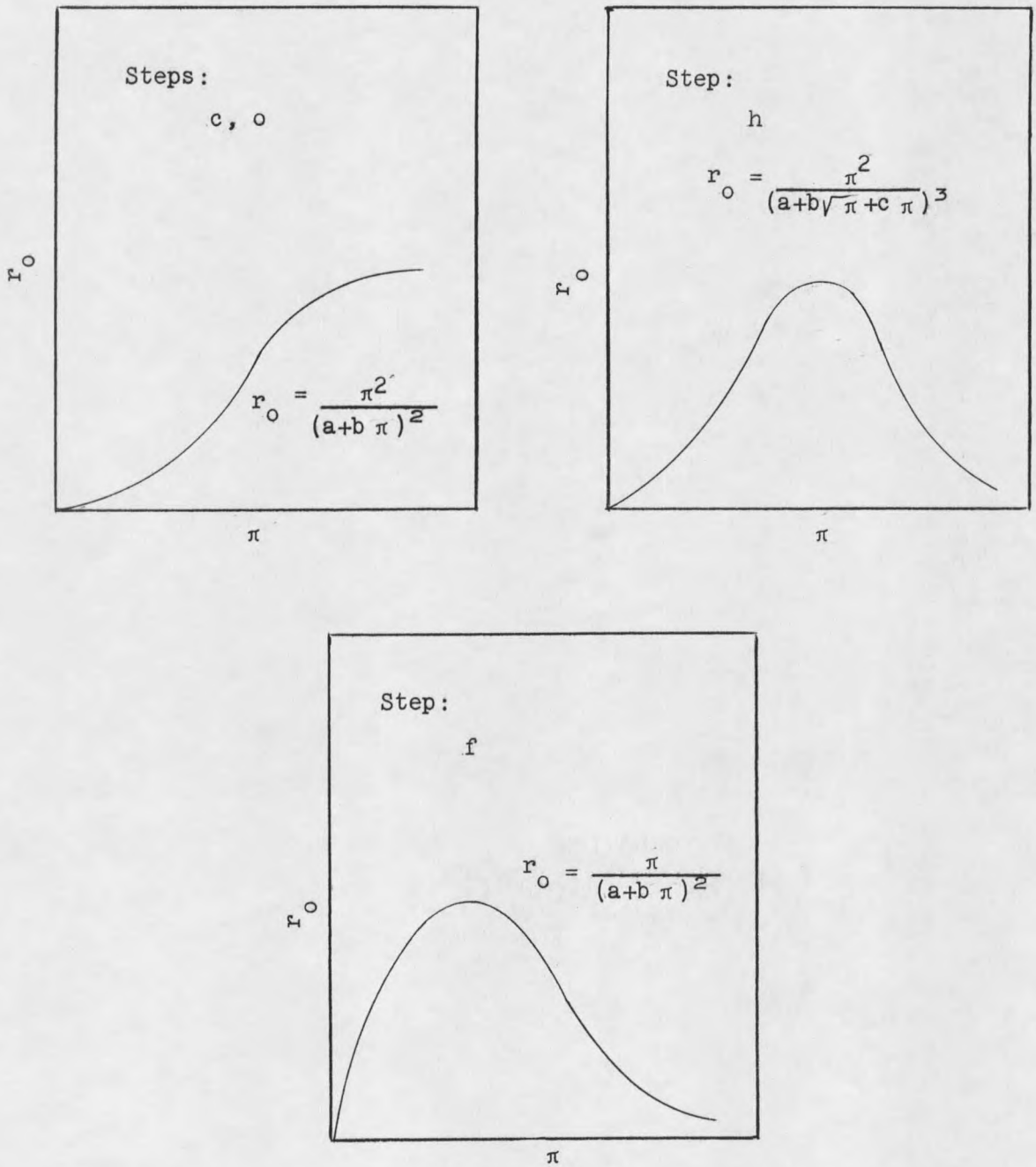

Figure 12 (cont.). Graphs of Initial Reaction Rate Equations for Each Step Rate Controlling

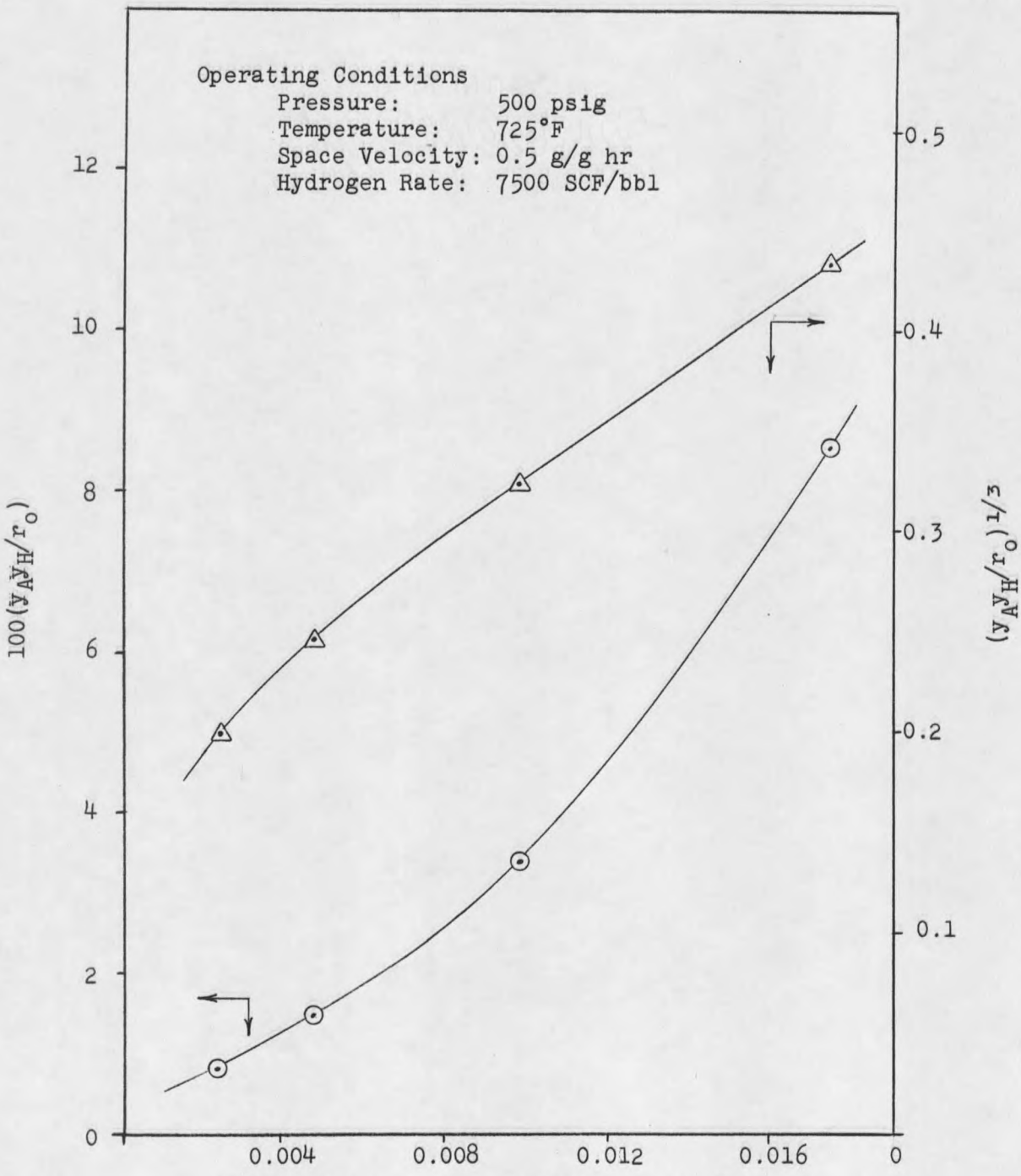

Figure 13. Plots of $y_A y_H / r_o$ and $(y_A y_H / r_o)^{1/3}$ vs. y_A for Checking Reaction Mechanism

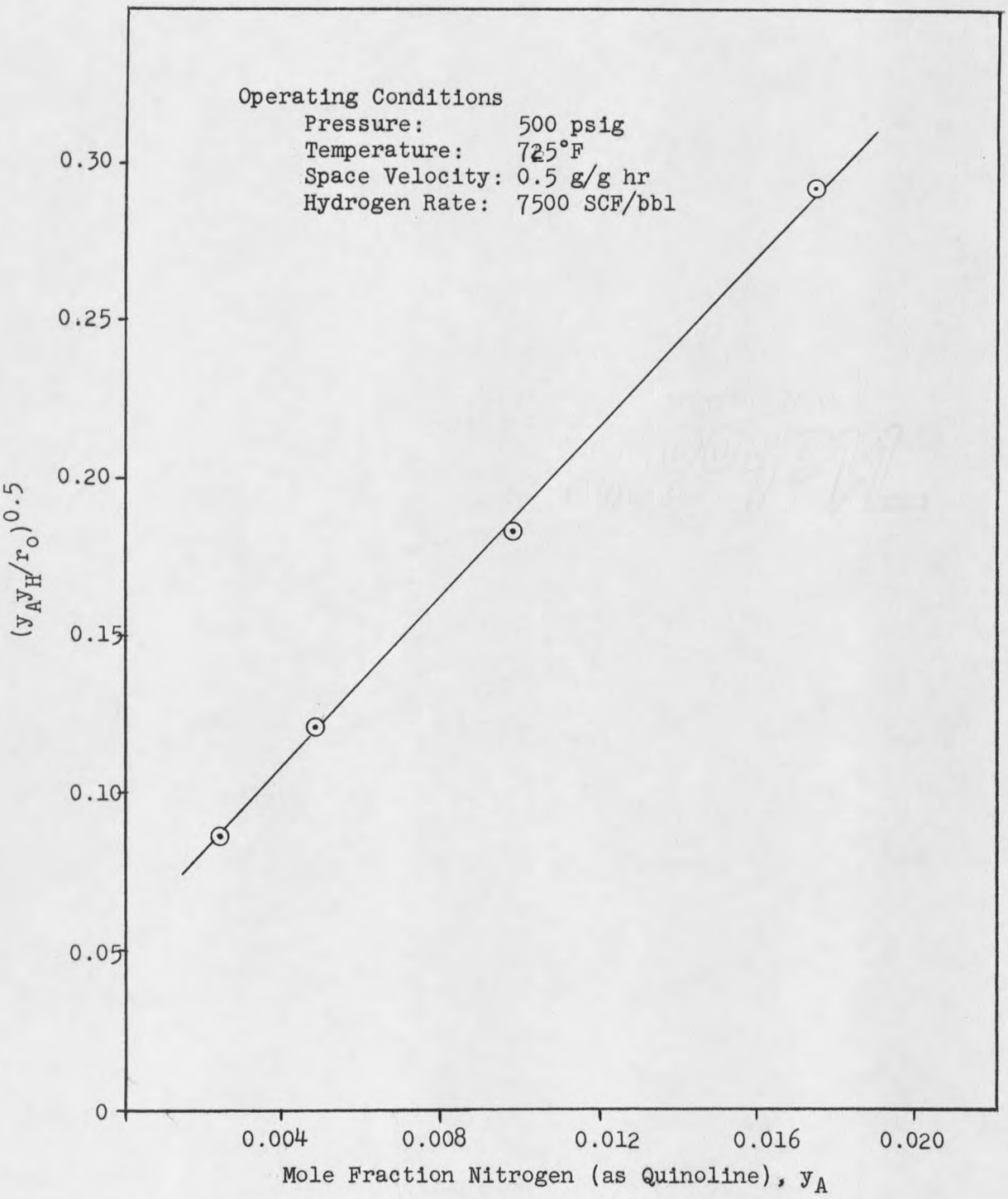

Figure 14. Plot of $(y_A y_H/r_o)^{0.5}$ vs. y_A for Checking Reaction Mechanism

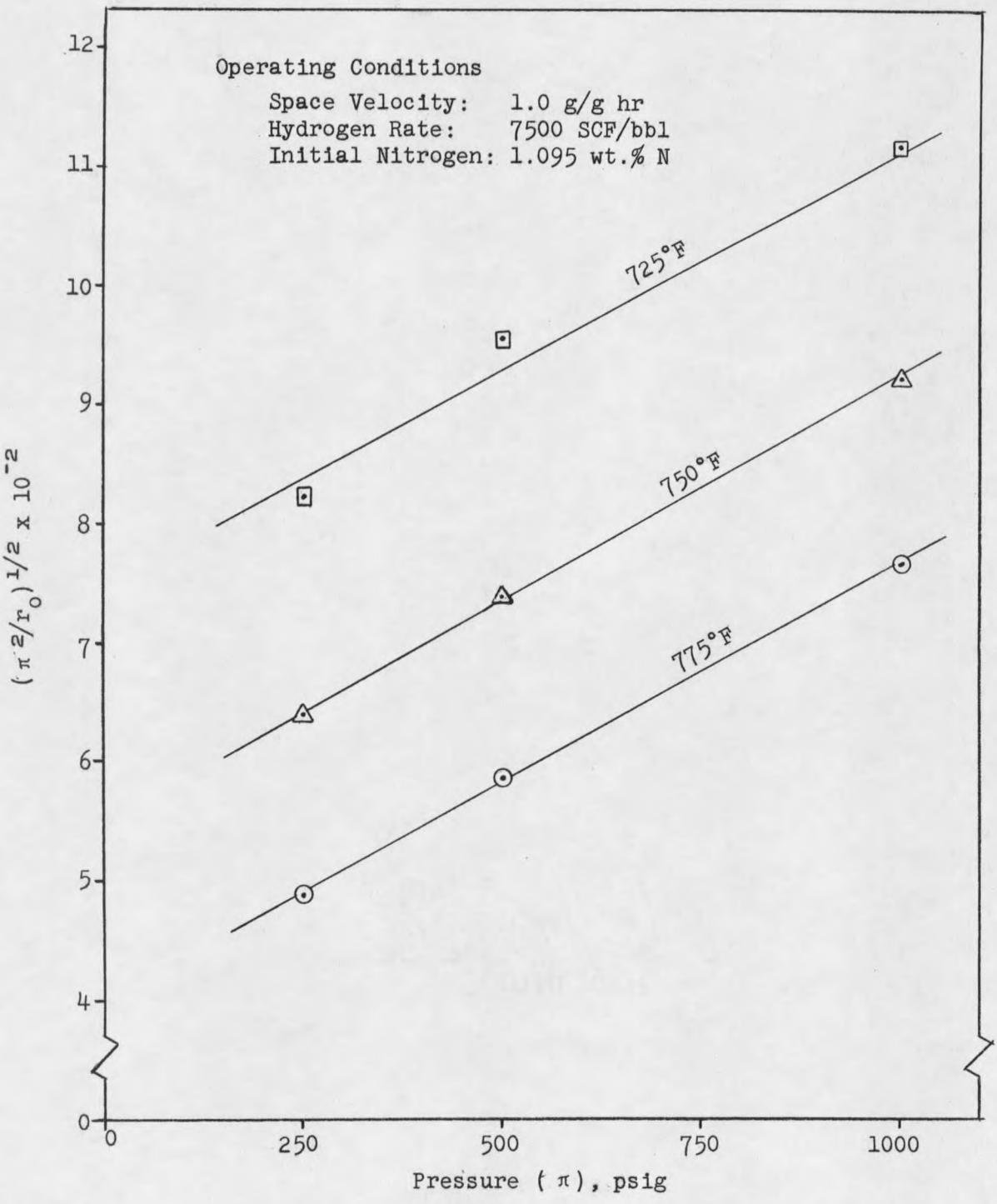

Figure 15. Plot of $(\pi^2/r_o)^{1/2}$ vs. Pressure to Check Reaction Mechanism

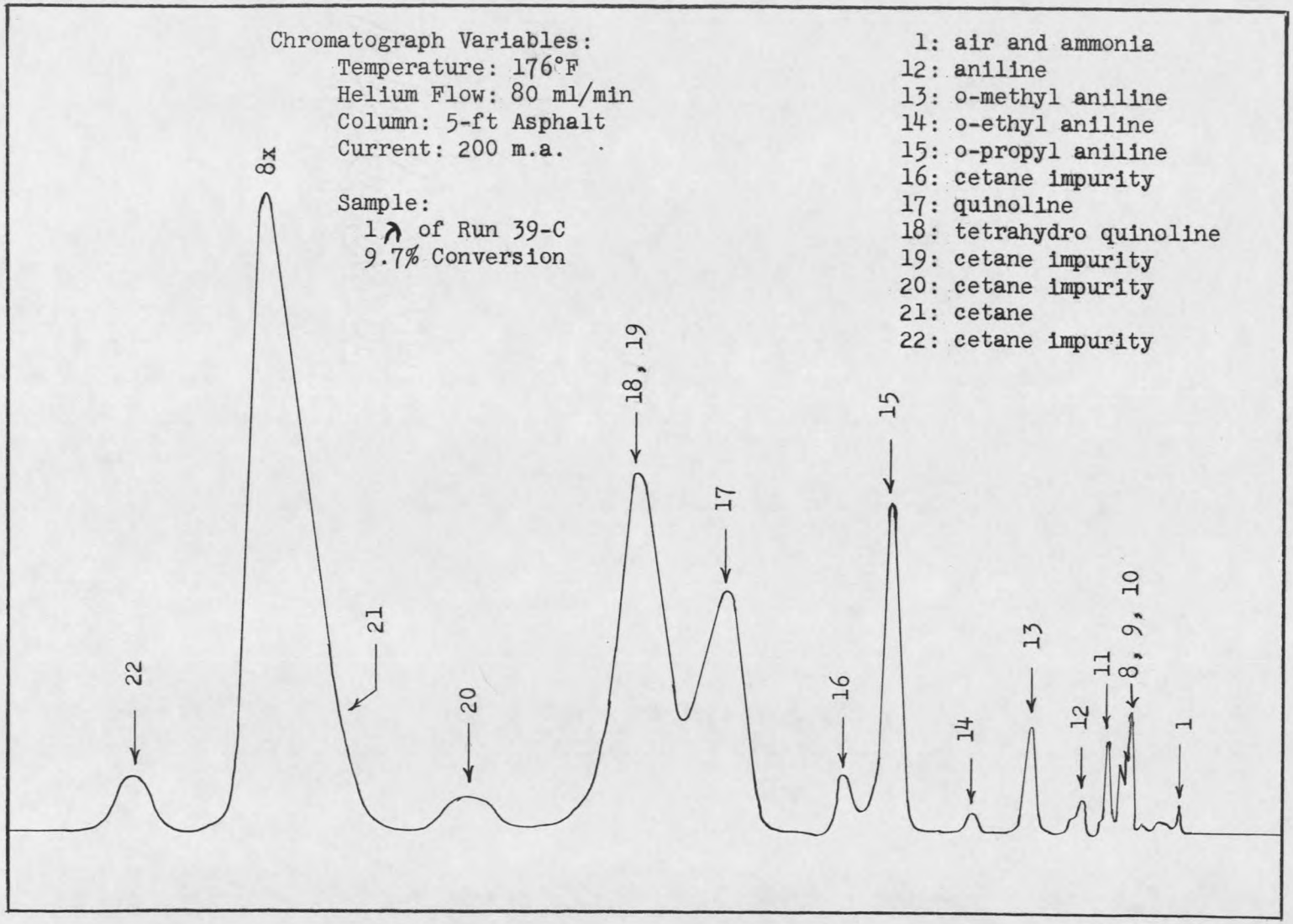

Figure 16. Chromatogram of Product from Run 39-C

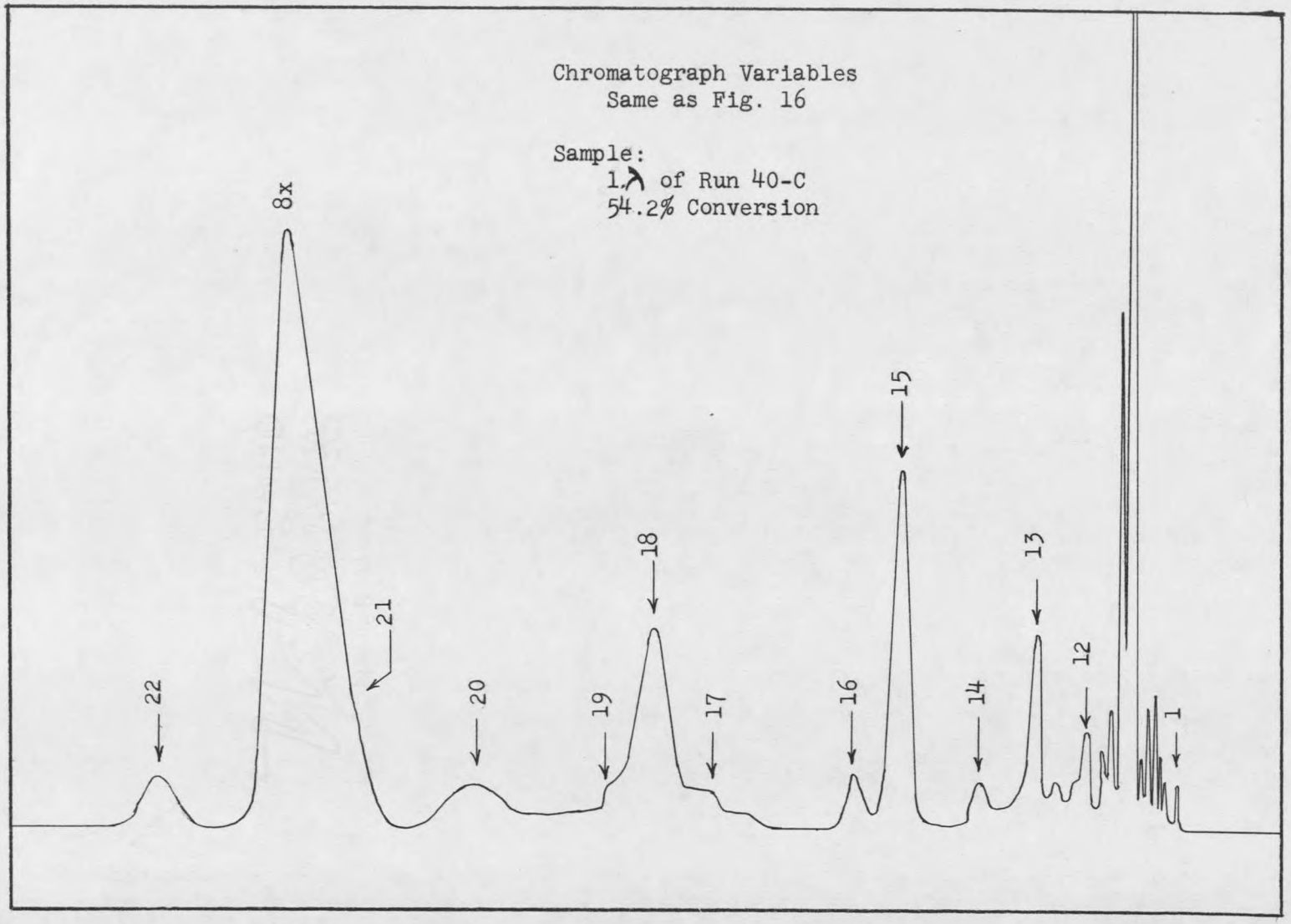

Figure 17. Chromatogram of Product from Run 40-C

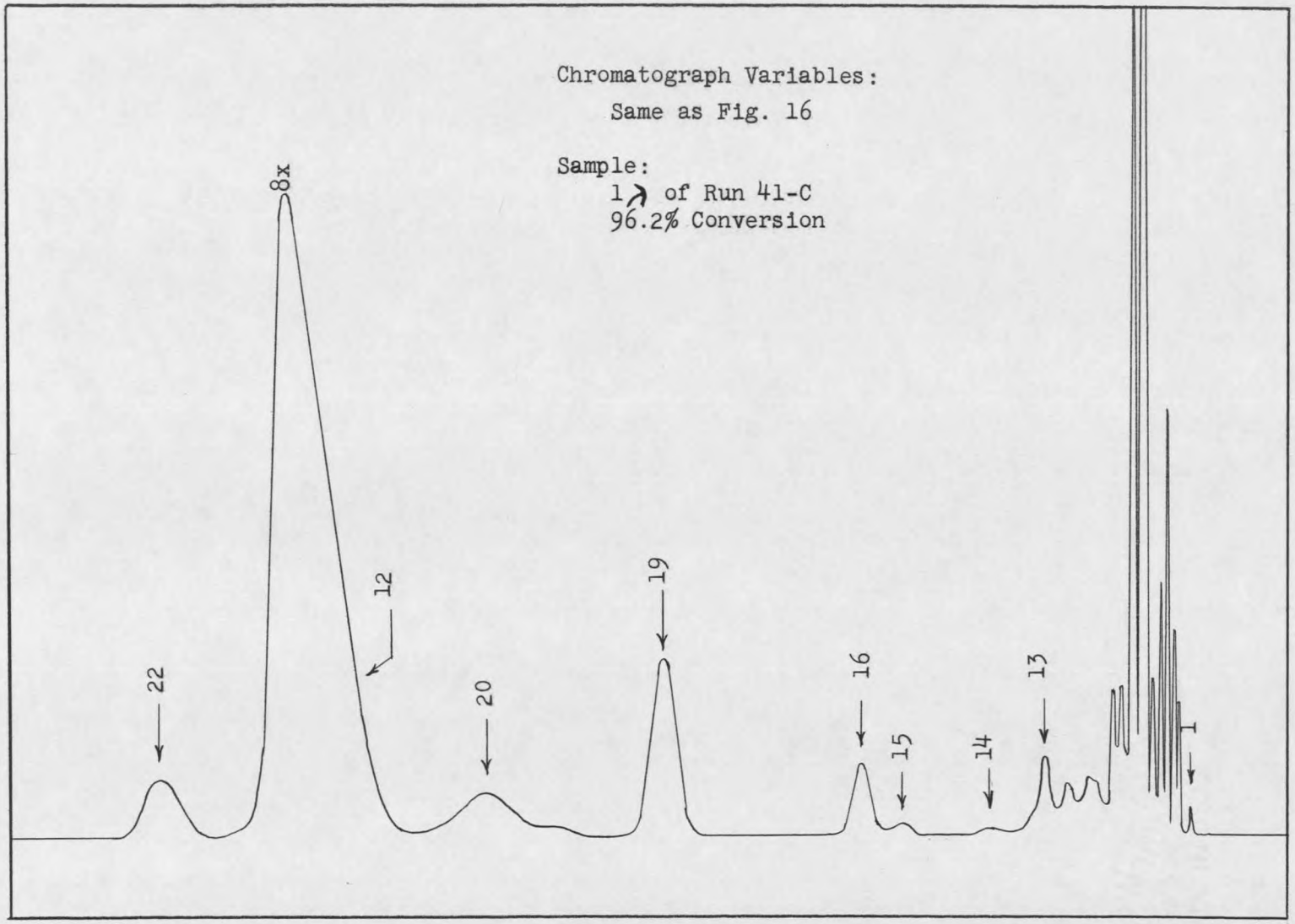

Figure 18. Chromatogram of Product from Run 41-C

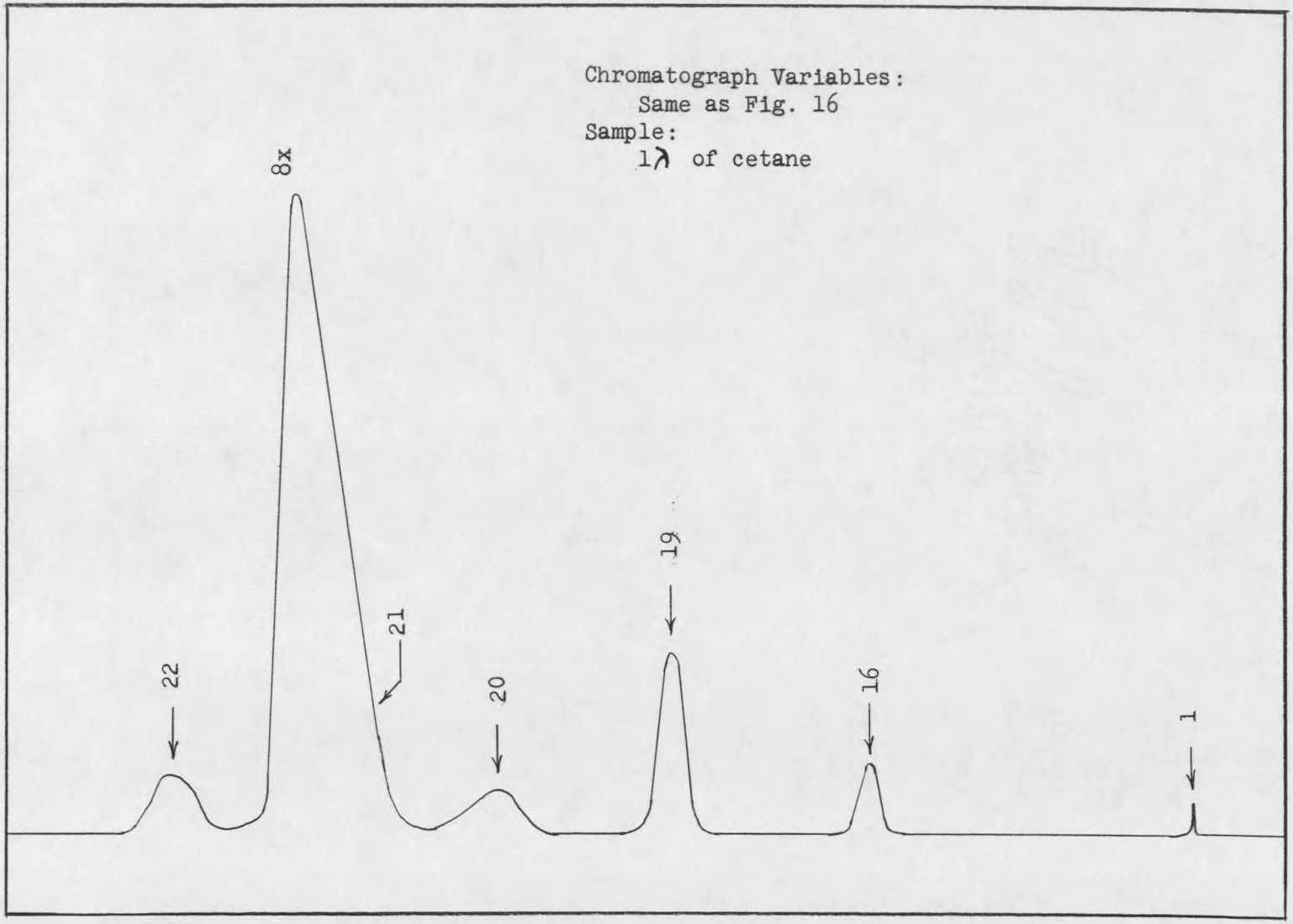

Figure 19. Chromatogram of Cetane

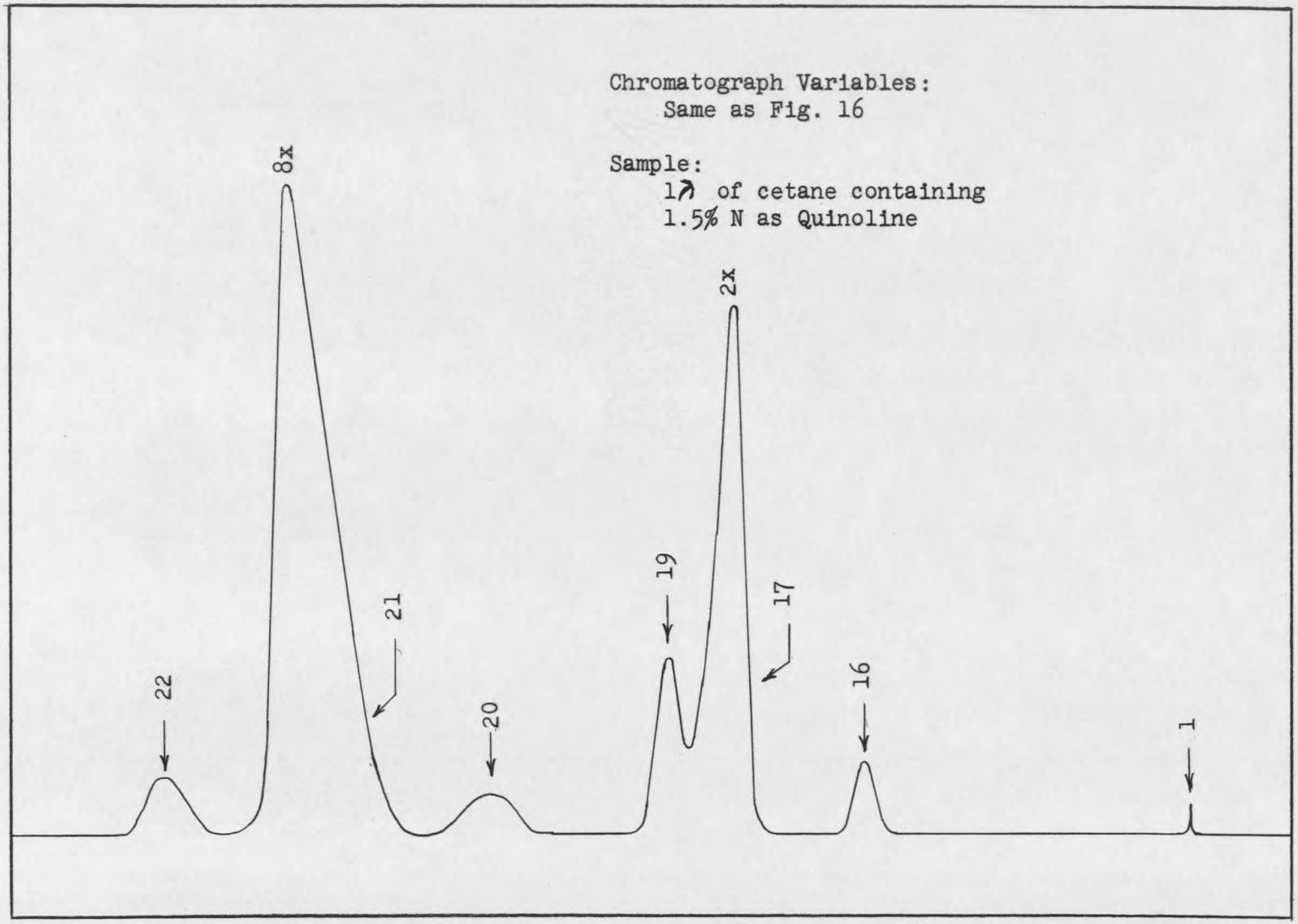

Figure 20. Chromatogram of Cetane-Quinoline Feed

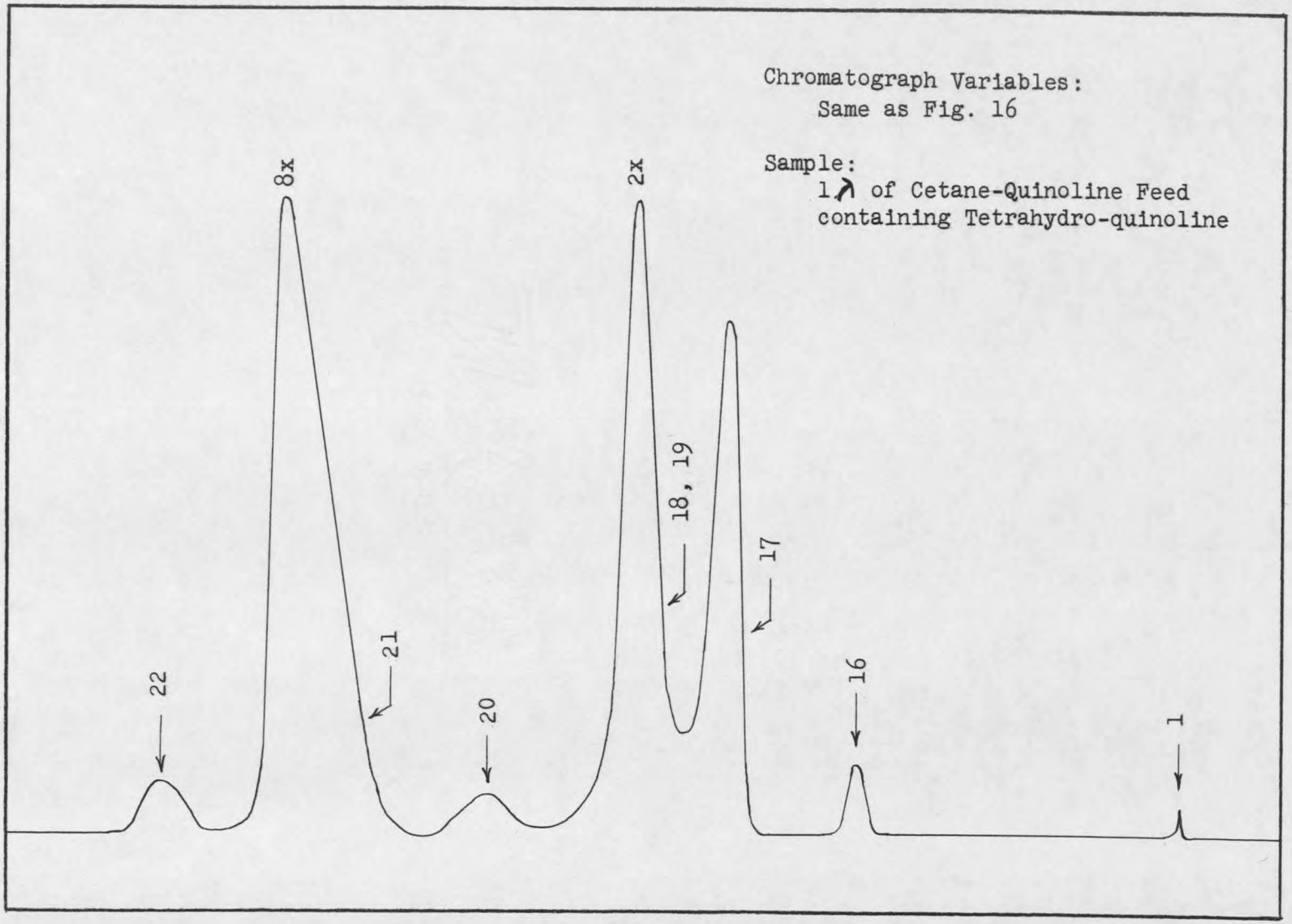

Figure 21. Chromatogram of Cetane-Quinoline Feed Containing Some Tetrahydro-quinoline

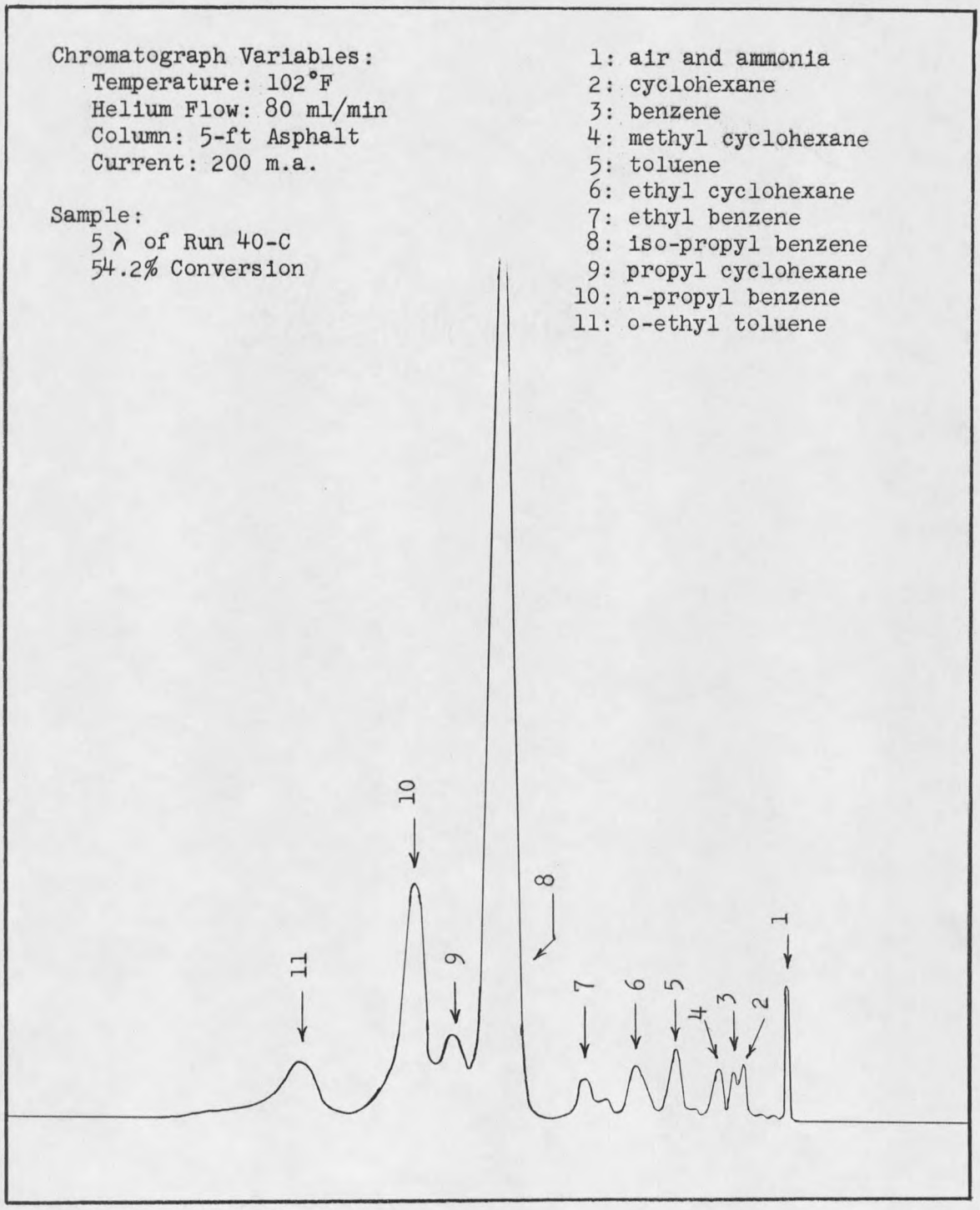

Figure 22. Chromatogram of Typical Product Distribution

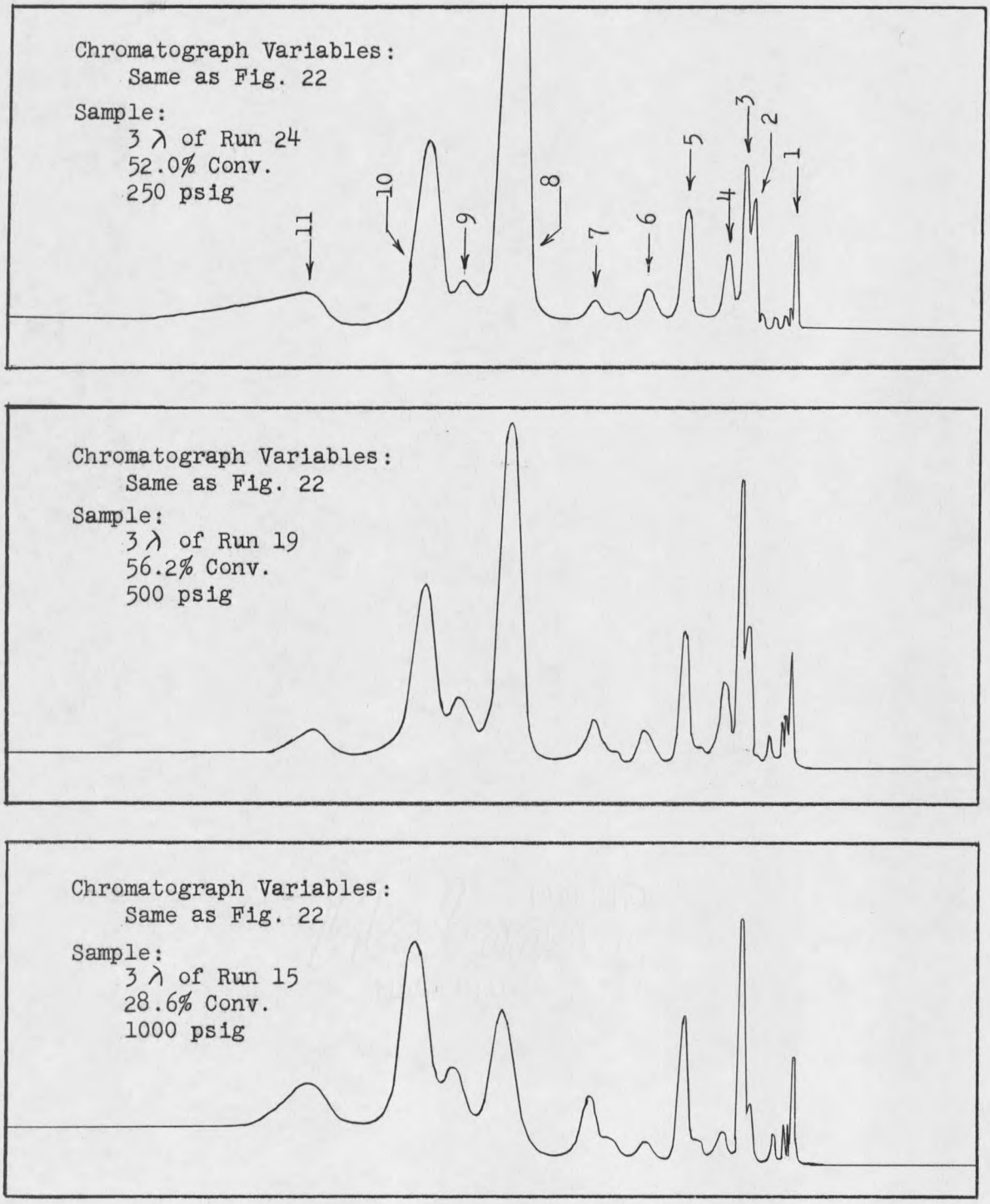

Figure 23. Chromatogram Showing Effect of Pressure on Product Distribution

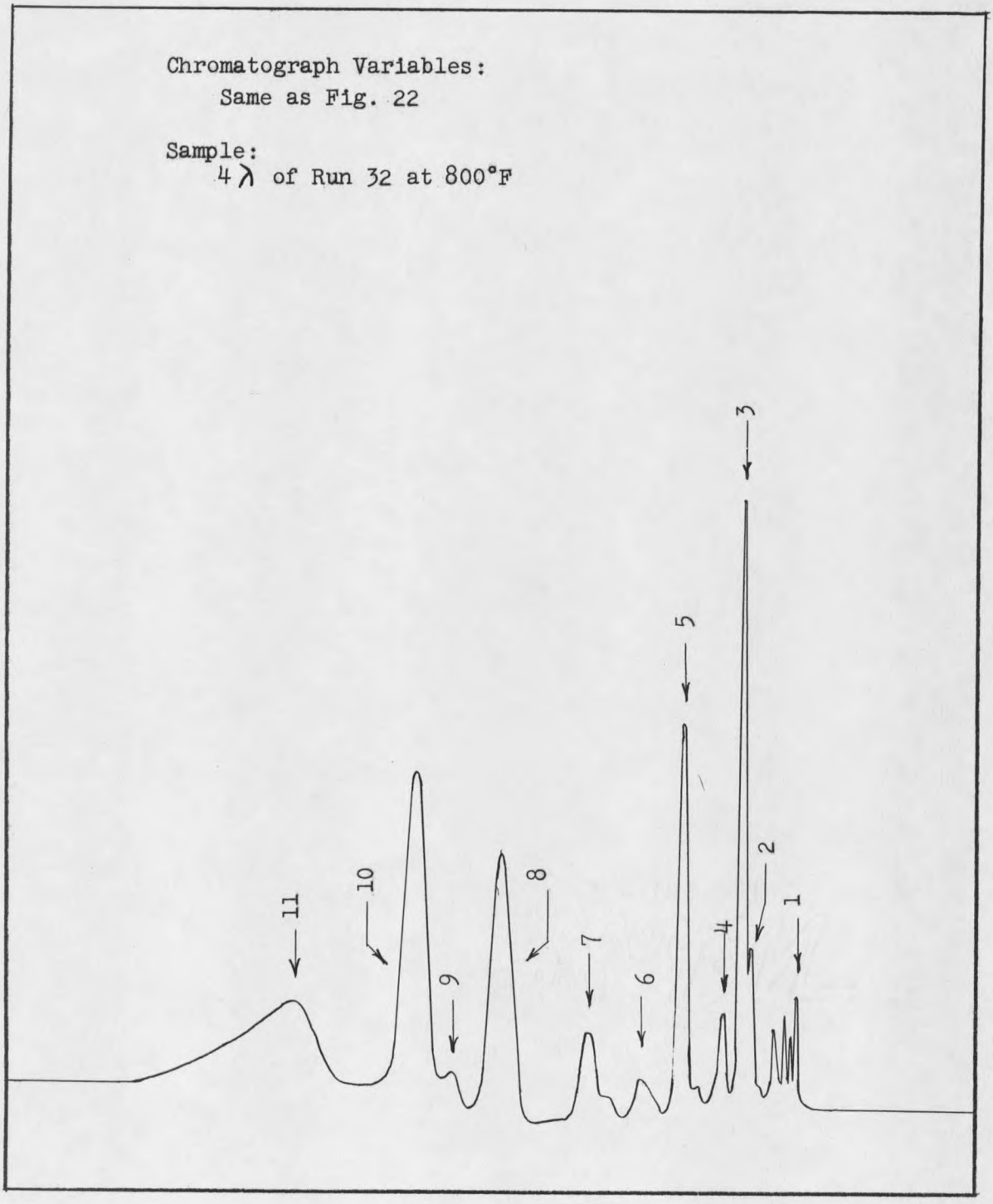

Figure 24. Chromatogram Showing Effect of Temperature on Product Distribution

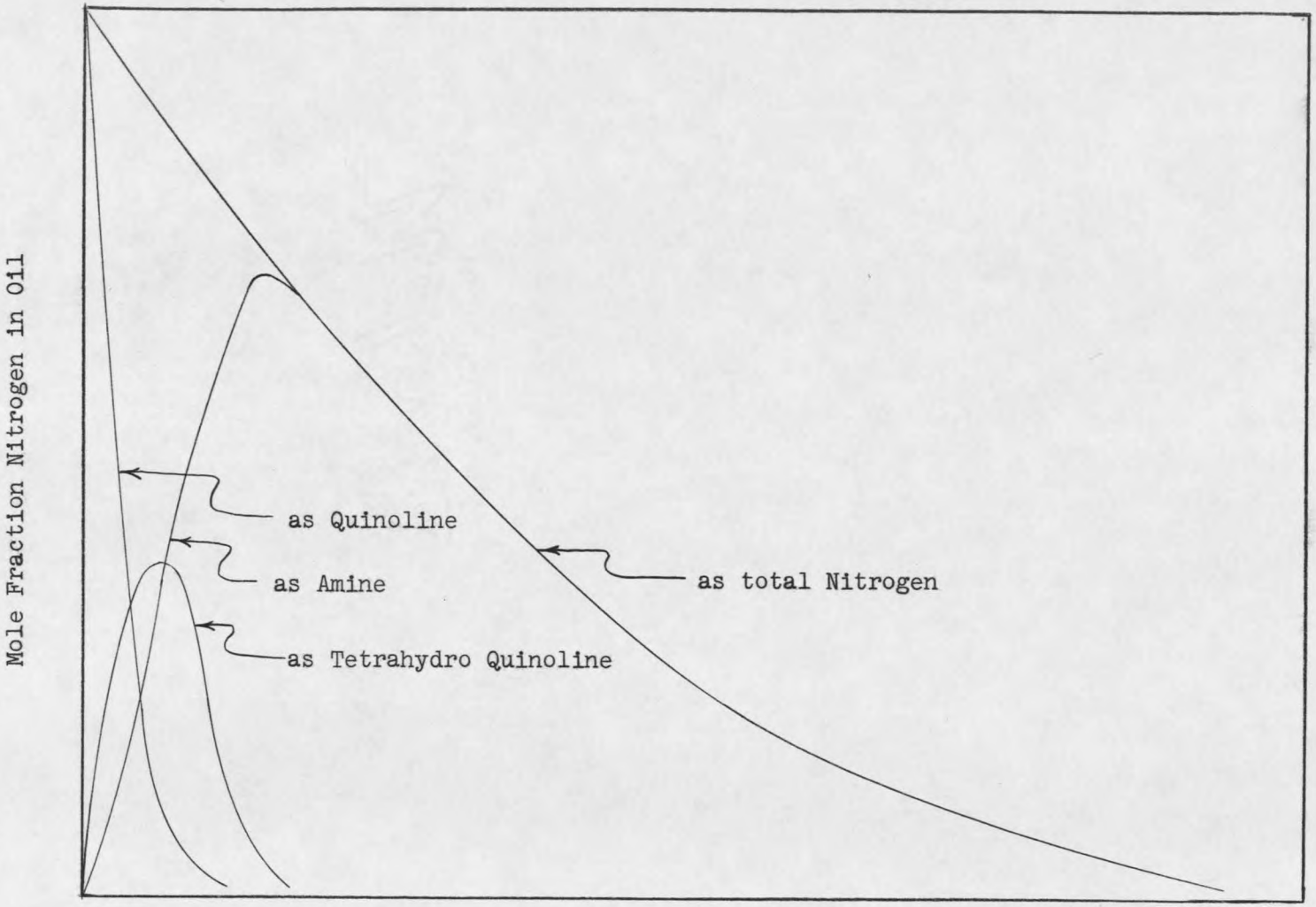

Figure 25. Simulated Nitrogen Distribution for the Hydrogenation of Quinoline

X VITA

PERSONAL

Date and Place of Birth: March 15, 1934
Great Falls, Montana

Marital Status: Married; 2 children

EDUCATIONAL

High School: Belt Valley High School, Belt, Montana;
9/48 to 6/52

Undergraduate: Montana State College, Bozeman, Montana;
9/52 to 6/56; B.S. in Chemical Engineering

Graduate: Fridericiana Technische Hochschule, Karlsruhe,
Germany; 9/56 to 6/57

Montana State College, Bozeman, Montana;
9/57 to 6/60

EXPERIENCE

Technologist with the Shell Chemical Corporation, Martinez,
California; 6/55 to 9/55

Research Fellow in Chemical Engineering, Montana State College,
Bozeman, Montana; 9/57 to 3/60

Graduate Assistant in Mathematics, Montana State College,
Bozeman, Montana; 9/57 to 3/60.